Master's thesis

NTNU
Norwegian University of Science and Technology
Faculty of Information Technology and Electrical Engineering
Department of Electronic Systems

Magnar Storflor

Comparison of ISO 10534-2 Versus Other Methods for Determining the Sound Absorption Coefficient of Materials in an Impedance Tube

Master's thesis in Electronics Systems Design and Innovation
Supervisor: Peter Svensson
June 2022

NTNU
Norwegian University of Science and Technology

Magnar Storflor

Comparison of ISO 10534-2 Versus Other Methods for Determining the Sound Absorption Coefficient of Materials in an Impedance Tube

Master's thesis in Electronics Systems Design and Innovation
Supervisor: Peter Svensson
June 2022

Norwegian University of Science and Technology
Faculty of Information Technology and Electrical Engineering
Department of Electronic Systems

NTNU

Kunnskap for en bedre verden

Comparison of ISO 10534-2 Versus Other Methods for Determining the Sound Absorption Coefficient of Materials in an Impedance Tube,
TFE4940

Master Thesis
June, 2022

Author:
Magnar Storflor

Published by: NTNU, Department of Acoustics, Norway
www.ntnu.no

PREFACE

This thesis the final result of the master's program "Electronics Systems Design and Innovation" at the Norwegian University of Science and Technology (NTNU). Work started late December 2021 and was concluded June 2022. Peter Svensson, who was the supervisor for this work, proposed the original idea for this thesis.

For the final part of the master's program, I decided to specialize in acoustics. I found out that I enjoyed building acoustics the most, and expected that I would be doing something quite different from what ended up happening for this master thesis.
I had already encountered measurements of absorption coefficients in a reverberation room for an unrelated project that was completed previously. So it seemed like a good idea to also get introduced to to the impedance tube method in depth as well.

Abstract

This thesis compares the method of the internationally recognized standard ISO 10534-2, "Determination of sound absorption coefficient and impedance in impedance tubes Part 2: Transfer function method (ISO 10534-2:1998)" (Method 0), with alternate methods that are also performed in an impedance tube. One such method uses 5 microphone positions to find potentially more accurate results by averaging these different positions (Method 1). Another method uses the least mean squares solution with 5 microphone positions (Method 2). The final method is a simplified one-dimensional reverberation-time-based method (Method 3). Different samples of varying reflection factors are used to see whether highly reflective or absorbing materials have an undesirable effect on any of the methods being tested.

The focus is mainly on the accuracy of measuring the reflection constant for highly reflective materials. A few methods that can be used to compensate for propagation loss is detailed in ISO 10534-2. It was however, not immediately apparent how this would be performed in an impedance tube with fixed microphone positions. For that reason a different method using several fixed microphone positions is implemented. The importance of compensating for propagation loss is shown, especially for highly reflective materials, as when calculating the absorption coefficient for the empty tube, non-compensated results were 125% larger on average for Method 0.

A small note regarding Method 3 is in order. Method 3 was found to have problems in the lower third-octave bands of the operating frequency range of the impedance tube. Method 3's reflection factor is the product of the reflection factor for the loudspeaker and the sample under test. By dividing a sample's reflection factor, measured by Method 3, with the reflection factor of the empty tube (Method 3), the influence of the loudspeaker was removed. This was compared to Methods 0, 1, and 2, doing a similar division of their reflection factors for the sample by the empty tube. This showcased the erroneous results in the lower frequency bands for Method 3, while higher bands followed the other Methods more closely. In addition, it was unclear how Method 3 would be compensated for attenuation. These, among other reasons, caused Method 3 to be excluded from any valid comparison with Method 0.

Method 0 was found to have a 70% larger average margin of error (t-value for the 95% confidence interval multiplied by the standard error) than Method 2, which had the lowest average margin of error for the empty impedance tube. For the high absorbing sample "glass wool 100mm", Method 0 had a 58% larger average margin of error than Method 1, which performed the best for the glass wool sample.

Reflection factors compensated for propagation attenuation using a line-fit for k" (attenuation constant) were used to calculate the absorption coefficients. This was done to compare the Methods, as Methods 1 and 2 use extra microphones further from the sample (and in addition to) than the ones used by Method 0. For the empty impedance tube, there was an average of 14.9% and 16.3% relative difference in the calculated absorption

coefficients for Method 1 and 2, respectively when compared to Method 1. This was reduced to 0.13% and 0.18% for Method 1 and 2 respectively, compared to Method 0. This means that if either Method 1 or 2 is more correct than Method 0; there is a non-negligible improvement for using those Methods instead of Method 0 for highly reflective samples. For high absorption samples, however, the difference in using Method 1 or 2 over Method 0 is hardly noticeable.

Sammendrag

Denne oppgaven sammenligner metoden til den internasjonalt anerkjente standarden ISO 10534-2, Bestemmelse av lydabsorpsjonsfaktor og impedans i impedansrør Del 2: Metode som bruker overføringsfunksjon (ISO 10534-2:1998)"(Metode 0), med alternative metoder som også utføres i et impedansrør. Én slik metode bruker 5 mikrofonposisjoner for å finne potensielt mer nøyaktige resultater ved å beregne gjennomsnittet av disse forskjellige posisjonene (Metode 1). En annen metode bruker løsningen for minste kvadraters metode med 5 mikrofonposisjoner (Metode 2). Den siste metoden er en forenklet endimensjonal etterklangstidsbasert metode (Metode 3). Ulike prøver med varierende refleksjonsfaktorer brukes for å se om sterkt reflekterende eller absorberende materialer har en uønsket effekt på noen av metodene som testes.

Fokuset er hovedsakelig på nøyaktigheten av å måle refleksjonskonstanten for svært reflekterende materialer. Noen få metoder som kan brukes for å kompensere for forplantningstap er beskrevet i ISO 10534-2. Det var imidlertid ikke umiddelbart klart hvordan dette ville bli utført i et impedansrør med faste mikrofonposisjoner. Av den grunn implementeres en annen metode som bruker flere faste mikrofonposisjoner. Viktigheten av å kompensere for forplantningstap er vist, spesielt for svært reflekterende materialer, da ved beregning av absorpsjonskoeffisienten for det tomme røret, var ikke-kompenserte resultater 125% større i gjennomsnitt for Metode 0.

En liten merknad angående Metode 3 er på sin plass. Metode 3 ble funnet å ha problemer i de nedre tredjedelsoktavbåndene i driftsfrekvensområdet til impedansrøret. Metode 3 sin refleksjonsfaktor er produktet av refleksjonsfaktoren for høyttaleren og prøven som testes. Ved å dele en prøve sin refleksjonsfaktor, målt med Metode 3, med refleksjonsfaktoren til det tomme røret, ble påvirkningen fra høyttaleren fjernet. Dette ble sammenlignet med Metode 0, 1 og 2, hvor en lignende dele operasjon av refleksjonsfaktorene for prøven delt på det tomme røret sin refleksjon faktor for hver enkelt metode. Dette viste frem de feilaktige resultatene i de lavere frekvensbåndene for Metode 3, mens høyere frekvensbånd fulgte de andre metodene nærmere. I tillegg var det uklart hvordan Metode 3 ville bli kompensert for demping. Disse, blant andre årsaker, gjorde at Metode 3 ble ekskludert fra enhver gyldig sammenligning med Metode 0.

Metode 0 ble funnet å ha en 70% større gjennomsnittlig feilmargin (t-verdi for 95% konfidensintervall multiplisert med standardfeilen) enn Metode 2, som hadde den laveste gjennomsnittlige feilmarginen for det tomme impedansrøret. For den høyabsorberende prøven glassull 100mm"hadde Metode 0 en 58% større gjennomsnittlig feilmargin enn Metode 1, som presterte best for glassullprøven.

Refleksjonsfaktorer kompensert for forplantningsdempning ved bruk av en linjetilpasning for k" (dempningskonstant) ble brukt for å beregne absorpsjonskoeffisientene. Dette ble gjort for å sammenligne metodene, da Metode 1 og 2 bruker ekstra mikrofoner lenger fra prøven (og i tillegg til) enn til de som ble brukt av Metode 0. For det tomme impedansrøret

var det gjennomsnittlig 14.9% og 16.3% relativ forskjell i de beregnede absorpsjonskoeffisientene for henholdsvis Metode 1 og 2 sammenlignet med Metode 1. Dette ble redusert til 0,13% og 0,18% for henholdsvis Metode 1 og 2, sammenlignet med Metode 0. Dette betyr at hvis enten Metode 1 eller 2 er mer riktig enn Metode 0; da er det en ikke ubetydelig forbedring ved å bruke Metode 1 eller 2, i stedet for Metode 0 for svært reflekterende prøver. For prøver med høy absorpsjon er imidlertid forskjellen i bruk av Metode 1 eller 2 i forhold til Metode 0 knapt merkbar.

ACKNOWLEDGEMENTS

Peter Svensson, Professor NTNU, Department of Electronic Systems:
Supervisor at NTNU

If not for Peter Svensson's kindness and willingness to help, combined with his wealth of knowledge and patience, this master thesis would not have been possible. Not only because of his role as a great supervisor and his support during my master thesis but also for his encouragement and aid through previous semesters. Beyond simply learning, my understanding of the field of acoustics has expanded thanks to him.
I would also like to thank my parents, whose endless love and support have motivated me over the years.
Thanks to my friends for their input and advice.

Thank you all very much!

CONTENTS

Preface ii
Abstract iii
Sammendrag v
Acknowledgements vii

1 Introduction **1**

2 Theory & Methods **3**
2.1 Two Microphone Technique 3
2.2 Influence of Propagation Loss 5
2.3 Experimental Methods to Determine Reflection Factor 7
2.3.1 Measurement of Impulse Response 7
2.3.2 Method 0, Two Microphone Positions ISO 8
2.3.3 Method 1, N > 1 Microphone Positions with Averaging 9
2.3.4 Method 2, N > 1 Microphone Positions with Least Mean Squares Method Solution 9
2.3.5 Method 3, Reverberation Time 11
2.3.6 The Speed of Sound and Temperature 13

3 Experiments **14**
3.1 Samples used 16
3.2 Processing 21

4 Results & Discussion **22**
4.0.1 Unique Attributes of Method 3 23
4.1 Reflection Factors Without Compensation For Propagation Attenuation . . 25
4.2 Influence of Compensating for Sound Attenuation 27
4.3 Reflection Factors Compensated for Sound Attenuation 30
4.4 Statistical Analysis 33
4.5 Absorption Coefficient α 36
4.6 Influence of Leakage 40

5 Conclusion **42**

Bibliography **44**

A Appendix **A**

CHAPTER

ONE

INTRODUCTION

As technology has advanced, new cost efficient, time efficient or otherwise improved methods have become available. One example of this in the world of acoustics is software developed in order to be able to simulate the acoustic environment of perhaps a room, even an entire building in the case of a building acoustician.

Pre-planning can be done using a computer to determine if a street or railway will be too noisy for nearby inhabitants and lets one know that noise barriers or some other solution may be needed.

In order to correctly model such situations it is of utmost importance to have accurate values for absorption coefficients. [**1**]

One such method is described in ISO 354:2003 "Measurement of sound absorption in a reverberation room" [**2**]. However, this reverberation room method can become quite cumbersome for certain materials as it requires 10 to 12 square meters [**2**] of the given sample to perform. An alternative to this method is ISO 10534-2 [**3**] "Determination of sound absorption coefficient and impedance in impedance tubes". This impedance tube method allows for comparatively much smaller samples and a drastically increased resolution for the measured absorption coefficient rather than just the one-third octave-band values.

Both methods mentioned have problems regarding accuracy when it comes to the measurement of highly reflective materials / materials with low absorption coefficients [**4**]. For the most part this is not an issue, as most of the time, interest is centered around highly absorbing materials for the purpose of sound insulation. Special cases exist however, such as modeling natural caves, tunnels or buildings comprised mainly of stone or glass like glass covered inner yards. For these kinds of locations, the materials present will primarily be highly reflective, and therefore, the accurate determination of the acoustic properties of such materials will be of great importance when modeling such places.

This paper will evaluate the method from ISO 10534-2, as well as variations of that method, one using averaging of different microphone positions, another, the least mean

squares based solution of multiple microphone positions, and finally, a T_{60} based reverberation time method in the impedance tube. There will be a particular focus on highly reflective materials, but a few absorbing materials will also be tested. The working frequency range will be 55-830Hz. In an attempt to see if it is possible to improve upon the current standard, these methods will be compared with their strengths and weaknesses. Absorption values will be calculated for each method, and the impact of propagation attenuation will be investigated for both highly reflective and high absorption materials. Statistical analysis will also be used in order to evaluate the different methods.

CHAPTER

TWO

THEORY & METHODS

2.1 Two Microphone Technique

The two microphone technique is a method used to find the reflection factor of a sample, which leads to the absorption factor of the sample. A graphical representation is shown in figure 2.1

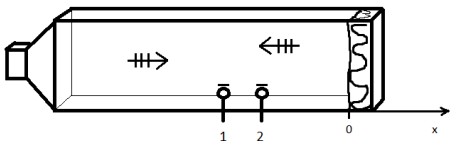

Figure 2.1: Impedance tube for the two microphone technique

In figure 2.1, the impedance tube is shown with a loudspeaker to the left, microphones 1 and 2 near the center, and a sample mounted on the right (terminating in a hard wall). It is assumed that only plane waves are propagating within the tube. This allows a simple 1D equation to describe the sound pressure within the tube, where the time-harmonic factor e^{jwt} is assumed.

$$p(\omega) = Ae^{-jkx} + Be^{jkx} \tag{2.1}$$

In equation 2.1, Ae^{-jkx} describes the plane wave traveling in the positive x-direction, and Be^{jkx} describes the wave traveling in the opposite direction, having been reflected from the sample. The $\hat{p}$ is the complex sound pressure amplitude resulting from the superposition of these two waves.

As stated previously, the technique's goal is to find the reflection factor of a sample, which is given by $R = \frac{B}{A}$ if the sample is placed at x = 0. To do this, the sound pressure amplitude is measured in two microphone locations. Using the measured sound pressure data collected from two microphone positions gives two equations with two unknowns, A

and R. Each equation will be in the form as shown in equation 2.2 for each microphone position.

$$p(\omega) = A(e^{-jkx} + \frac{B}{A}e^{jkx})$$

$$p(\omega) = A(e^{-jkx} + Re^{jkx}) \tag{2.2}$$

By dividing p_1 by p_2 (the two sound pressure amplitudes measured in positions 1 and 2, respectively), A is eliminated and an expression results with R as the only unknown. Figure 2.2 in combination with equations 2.3 and 2.4 shows how this is done.

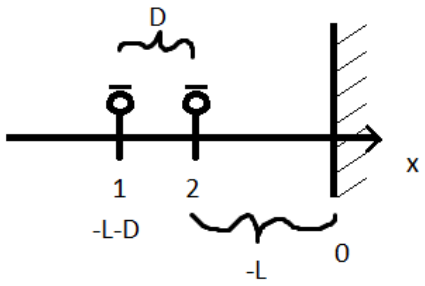

Figure 2.2: Impedance tube for the two microphone technique

In figure 2.2, L is the distance from the hard wall (or surface to the test sample) to microphone 2, and D is the distance between microphone 1 and 2. It is essential to notice the negative signs due to how the x-axis is defined.

$$\frac{p_1}{p_2} = \frac{A[e^{-jk(-L-D)} + Re^{jk(-L-D)}]}{A[e^{-jk(-L)} + Re^{jk(-L)}]}$$

$$\frac{p_1}{p_2} = \frac{e^{-jk(-L-D)} + Re^{jk(-L-D)}}{e^{-jk(-L)} + Re^{jk(-L)}}$$

$$\frac{p_1}{p_2} = \gamma = \frac{e^{2jkL} \cdot e^{jkD} + Re^{-jkD}}{e^{2jkL} + R} \tag{2.3}$$

Which then leads to equation 2.4:

$$R = -e^{2jkL} \cdot \frac{\gamma - e^{jkD}}{\gamma - e^{-jkD}} \tag{2.4}$$

Equation 2.4 shows the final result and can be used to find the reflection factor R. [**3**]

2.2 Influence of Propagation Loss

The derivation in section 2.1 was done with the assumption that there will be no losses as the plane wave propagates in the tube. Realistically, there will be losses, though they can be considered negligible in many cases, especially for materials with medium to high absorption. Due to how the absorption coefficient α is related to the reflection factor, a rather large error can be introduced when calculating the absorption coefficient with very high reflection factors. ISO 10534-2 is a method used to determine the absorption coefficient after all, so this should be kept in mind.
Equation 2.5 shows how the absorption coefficient is calculated from the reflection factor:

$$\alpha = 1 - |R_{measured}|^2 \tag{2.5}$$

Consider a case where an empty tube is known to have a reflection factor of 0.99 and a highly absorbing sample is known to have a reflection factor of 0.1, and there is a propagation loss of 1%. The measured value will be a combination of the true reflection factor of the wall/sample and the propagation loss as seen in equation 2.6:

$$\alpha = 1 - |R_{empty|sample}|^2 \cdot |\mathrm{e}^{-\delta x}|^2 \tag{2.6}$$

Table 2.1 shows the error of α for this extreme case using equation 2.6.

True R factor	**True** α	**Calculated** α	**Error compared to true** α
0.1	0.9900	0.9902	0.02%
0.5	0.7500	0.7500	0.00%
0.99	0.0199	0.0394	97.99%

Table 2.1: The measured α error from highly absorbing material versus highly reflective wall

Multiple factors cause sound attenuation. The viscosity of air, heat conduction, boundary effects, and relaxation processes. This is explained in detail in [**5**], but very briefly in the following points:

- Portions of the energy of a plane wave are transformed into thermal energy at regions of high pressure, and that heat is in turn transferred to low-pressure areas.
- Directly next to a boundary, air particles will not move. A transitional area extends out from a boundary, which impedes the particles less and less the further away from the boundary they are.
- Changes to temperature or pressure disturb the equilibrium of the different molecules that air is made up of. This causes loss which remains until a new equilibrium is established.

But the total sound attenuation can be represented as in ISO 10534-2 [**3**], with a complex wave number:

$$k_0 = k_0^{'} - jk_0^{''} \tag{2.7}$$

In equation 2.7, the wave number k_0 is changed to the complex wave number where $k_0^{''}$ is the sound attenuation coefficient which determines the exponential decay, with distance, of the propagating sound wave. This can be seen more easily when performed on a plane wave moving in the positive x-direction as in equation 2.8:

$$e^{-jk_0^{'}x} \cdot e^{-k_0^{''}x} \tag{2.8}$$

Having replaced k_0 with the complex number shows that the equation for the plane wave essentially stays the same but is now multiplied by a non-complex number (for a given frequency) $e^{-k_0^{''}x}$, the exponential loss.
One way to measure this attenuation factor experimentally is to use two pairs of microphone positions, the distance between each pair being equal. This is shown in figure 2.3.

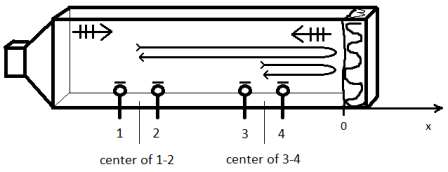

Figure 2.3: Figure illustrating the difference in distance travelled of the plane wave between measurements for two microphone pairs

One microphone pair measures close to the sample (within the guidelines of the standard). The other pair is further away from the sample, though not too close to the loudspeaker, where the plane wave assumption does not hold. The further away a microphone pair is, the more distance must be covered, hence greater attenuation. Equations 2.9 and 2.10 show how to find $k_0^{''}$:

$$\frac{|R_{close}|}{|R_{far}|} = \frac{|R_{true}| \cdot e^{-k_0^{''}2(D_{close})}}{|R_{true}| \cdot e^{-k_0^{''}2(D_{far})}} \tag{2.9}$$

$$k_0^{''} = \frac{-1}{2(D_{close} - D_{far})} \cdot \ln(\frac{|R_{close}|}{|R_{far}|}) \tag{2.10}$$

Here R_{close} is the measured reflection coefficient for the microphone pair placed closer to the sample. R_{far} is the measured reflection coefficient for the microphone pair placed further from the sample.R_{true} is the actual reflection coefficient without attenuation. D_{close} and D_{far} are the distances from the center point of the microphone pair closest and furthest from the sample, respectively.
Having determined k" one can now remove the influence of propagation attenuation:

$$R_{measured} = R_{true} \cdot e^{-k_0^{''}x}$$

Since the measured reflection factor is affected by the propagation attenuation given by $e^{-k_0^{''}}$, multiplying with its inverse should remove it and find the true value for the reflection factor. This is shown in equation 2.11:

$$R_{true} = R_{measured} \cdot e^{k_0'' x} \tag{2.11}$$

Here x will be the distance traveled that requires compensating as indicated in figure 2.3 with "U" shaped arrows. In this case, it will be 2 times the length from the center of the microphone pairs to the sample/wall.

A method of measuring the tube attenuation is mentioned in Annex A in ISO 10534-2 (A.2.1.3) [**3**] "Two pressure minima method" but it is unclear how this will be done with just two microphone positions.

2.3 Experimental Methods to Determine Reflection Factor

2.3.1 Measurement of Impulse Response

A sound signal $x(t)$ from the loudspeaker is sent through the impedance tube, which is assumed to be a linear time-invariant system. The resulting signal $y(t)$ is recorded using microphones in the tube. This output signal is the convolution of the input signal with the impulse response (the system). This is depicted in figure 2.4:

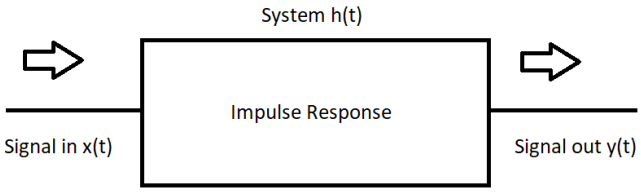

Figure 2.4: Simple schematic of impulse response

Equation 2.12 shows the mathematical relationship between the signal in, $x(t)$, the impulse response, $h(t)$, and the signal out, $y(t)$, where $*$ in this case is the convolution operator:

$$x(t) * h(t) = y(t) \tag{2.12}$$

In order to determine the unknown impulse response $h(t)$, FFT is used on both $x(t)$ and $y(t)$ to go from the time domain to the frequency domain and find $X(\omega)$ and $Y(\omega)$ respectively. Equation 2.13 shows the frequency domain equivalent of equation 2.12:

$$X(\omega) \cdot H(\omega) = Y(\omega) \tag{2.13}$$

$X(\omega)$ can be multiplied rather than convolved with the frequency response $H(\omega)$, and this will equal $Y(\omega)$. The frequency response can now easily be found through the division. Finally, by taking the inverse FFT of the frequency response, the system's impulse response is found.

The output signals $Y(\omega)$, which is the FFT of the signal out, $y(t)$ correspond to the sound pressure amplitudes p_i shown in section 2.1. When performing a practical measurement it

is normally the impulse response $h(t)$ which is measured. By using the impulse responses from the microphone measurements from microphone 1 and 2, and by taking the FFT of the impulse response for each microphone,one finds $H_i(\omega)$. By using $H_1(\omega)$ and $H_2(\omega)$ and dividing using equation 2.13 for microphone 1 and dividing by the same for microphone two, $X(\omega)$ can be eliminated (as the signal in is the same for both microphones) shown in equation 2.14.

$$\frac{X_1(\omega) \cdot H_1(\omega) = Y_1(\omega)}{H_2(\omega) \cdot H_2(\omega) = Y_2(\omega)}$$

$$\frac{H_1(\omega) = Y_1(\omega)}{X_2(\omega) = Y_2(\omega)} \tag{2.14}$$

One is then left with the ratio $\frac{H_1(\omega)}{H_2(\omega)}$ being equal to $\frac{p_1}{p_2} = \gamma$ mentioned in equation 2.3 which is used to solve for the reflection factor in equation 2.4.

2.3.2 Method 0, Two Microphone Positions ISO

This method of determining the absorption/reflection factor is described at length in ISO 10534-2 [**3**], a summarized version of important information will be provided in this section, however. The impedance tube may be circular or rectangular. Since the impedance tube used was rectangular, only formulas relevant to rectangular tubes will be shown here. The ISO mentions that areas too close to the loudspeaker or the sample can not be used as microphone positions, as shown in figure 2.5.

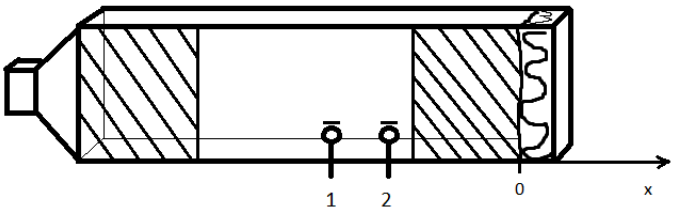

Figure 2.5: Covered areas represent unsuitable microphone positions (not to scale)

As this method assumes plane wave propagation, care must be taken not to have a microphone placed too close to either the loudspeaker or the sample. This is so that non-plane wave modes have time to die out.

At least three times the maximum lateral dimension is recommended for the distance between the loudspeaker and a microphone position. The microphone position in regards to the sample can vary from one-half maximum lateral dimension of the tube to two times depending on how structured or symmetrical the sample is. If the microphone is placed three maximum lateral dimensions away or more, corrections due to attenuation must be made. More details regarding this are available in section 2.2.
There is a working frequency range with a lower limit depending on the signal processing equipment used, and an upper limit that can be determined using equation 2.15:

$$f_{upper} < \frac{0.50 \cdot c_0}{d} \tag{2.15}$$

Here $f_{upper}$is the upper limit for the frequency range for the impedance tube, d is the maximum side length, and c_0 is the zero-frequency speed of sound.

The distance between the two microphone positions can be found using equation 2.16:

$$s < \frac{0.45 \cdot c_0}{f_{upper}} \tag{2.16}$$

Here s is the distance between two microphones used to determine the reflection factor.

A correction needs to be applied if two different microphones are used due to microphone differences. However, only one is used in this case.

2.3.3 Method 1, N > 1 Microphone Positions with Averaging

Method 1 is mostly similar to Method 0. The main difference is that multiple microphone pairs can hopefully achieve more accurate results using the mean measurement from multiple microphone pairs. All pairs used have the same distance between them.
Using this method, most microphone pair positions will be further away from the sample than recommended in the standard, and correction for attenuation will be required. If correction is not used, the results for the reflection factor will be reduced more and more the further the microphone pair is from the sample, skewing the estimated result away from the true value.

2.3.4 Method 2, N > 1 Microphone Positions with Least Mean Squares Method Solution

Method 2 is looking to solve equation 2.1 just as Methods 0 and 1. However, in this case, the best fit for an overdetermined set of equations is found instead. One way to do this is by setting up the N equations in matrix form as in equation 2.17 with N = 5:

$$\begin{bmatrix} e^{-jkx_1} & e^{jkx_1} \\ e^{-jkx_2} & e^{jkx_2} \\ e^{-jkx_3} & e^{jkx_3} \\ e^{-jkx_4} & e^{jkx_5} \\ e^{-jkx_5} & e^{jkx_5} \end{bmatrix} \begin{bmatrix} A \\ B \end{bmatrix} = \begin{bmatrix} p(x_1) \\ p(x_2) \\ p(x_3) \\ p(x_4) \\ p(x_5) \end{bmatrix} \tag{2.17}$$

A more compact version of equation 2.17 is shown in equation 2.18:

$$\mathbb{H} \begin{bmatrix} A \\ B \end{bmatrix} = \mathbb{P} \tag{2.18}$$

The next step is to solve for A and B. This is as the reflection coefficient can be found by dividing the amplitude of the reflected wave by the amplitude of the incoming wave. If the $\mathbb{H}$ matrix was square, this could be simply done by finding its inverse and multiplying on both sides. Software such as Matlab can compute the Moore-Penrose inverse [**6**], also known as the pseudoinverse. This can be used to solve for A and B to find the least mean squares solution, shown in equation 2.19.

$$\begin{bmatrix} A \\ B \end{bmatrix} = (\mathbb{H}^T\mathbb{H})^{-1}\mathbb{H}^T\mathbb{P}$$

$$\begin{bmatrix} A \\ B \end{bmatrix} = \mathbb{H}^+\mathbb{P} \tag{2.19}$$

Here, $^+$ in $\mathbb{H}^+$, is the notation for pseudoinverse. For any frequency, the reflection coefficient R can now be found as previously stated: $R = \frac{B}{A}$.

To account for sound attenuation, the first thought was to think of all the e^jkx parts of the equation actually being in the form as in 2.8 for the wave traveling in the positive x-direction, and the same but with negative signs removed for the negative direction. If $e^{-jk_0^{'}x} \cdot e^{-k_0^{''}x}$ is the model with loss in the positive x direction, then multiplying with $e^{k_0^{''}x}$ should remove the influence of the sound attenuation. Equation 2.20 shows the changes made to the matrix, by multiplying $e^{k_0^{''}x}$ to account for loss in the positive x-direction and $e^{-k_0^{''}x}$ to account for loss in the negative x-direction:

$$\begin{bmatrix} A \\ B \end{bmatrix} = \begin{bmatrix} e^{-jk_0^{'}x_1}e^{k_0^{''}x_1} & e^{jk_0^{'}x_1}e^{-k_0^{''}x_1} \\ e^{-jk_0^{'}x_2}e^{k_0^{''}x_2} & e^{jk_0^{'}x_2}e^{-k_0^{''}x_2} \\ e^{-jk_0^{'}x_3}e^{k_0^{''}x_3} & e^{jk_0^{'}x_3}e^{-k_0^{''}{}_3x} \\ e^{-jk_0^{'}x_4}e^{k_0^{''}x_4} & e^{jk_0^{'}x_5}e^{-k_0^{''}x_4} \\ e^{-jk_0^{'}x_5}e^{k_0^{''}x_5} & e^{jk_0^{'}x_5}e^{-k_0^{''}x_5} \end{bmatrix}^+ \mathbb{P} \tag{2.20}$$

Important note! The final part of this subsection details changes that had to be made to equation 2.20 to account for sound attenuation.

The expected result of 2.20 did not seem to give the correct answers. Having measured the value of $k_0^{''}$ experimentally using method 0, it turned out that equation 2.21 gave much more plausible results. Here the negative signs on the corrective factors have been switched.

$$\begin{bmatrix} A \\ B \end{bmatrix} = \begin{bmatrix} e^{-jk_0' x_1} e^{-k_0'' x_1} & e^{jk_0' x_1} e^{k_0'' x_1} \\ e^{-jk_0' x_2} e^{-k_0'' x_2} & e^{jk_0' x_2} e^{k_0'' x_2} \\ e^{-jk_0' x_3} e^{-k_0'' x_3} & e^{jk_0' x_3} e^{k_0''_3 x} \\ e^{-jk_0' x_4} e^{-k_0'' x_4} & e^{jk_0' x_5} e^{k_0'' x_4} \\ e^{-jk_0' x_5} e^{-k_0'' x_5} & e^{jk_0' x_5} e^{k_0'' x_5} \end{bmatrix}^{+} \mathbb{P} \tag{2.21}$$

Why the changes to the negative signs are necessary has not been fully understood. However, it is possibly due to how the x-axis is designed, as seen in figure 2.1, with the sample at x = 0 and microphones at negative x positions. When comparing propagation attenuation compensated results from method 0 and method 2, it is obvious that the negative signs must be switched. Otherwise, it compensates the reflection factor in the wrong y-direction. Equation 2.21 is the equation that has been used for method 2 to generate the reflection factors that are compensated for sound attenuation.

2.3.5 Method 3, Reverberation Time

Figure 2.6 illustrates the thought process behind Method 3:

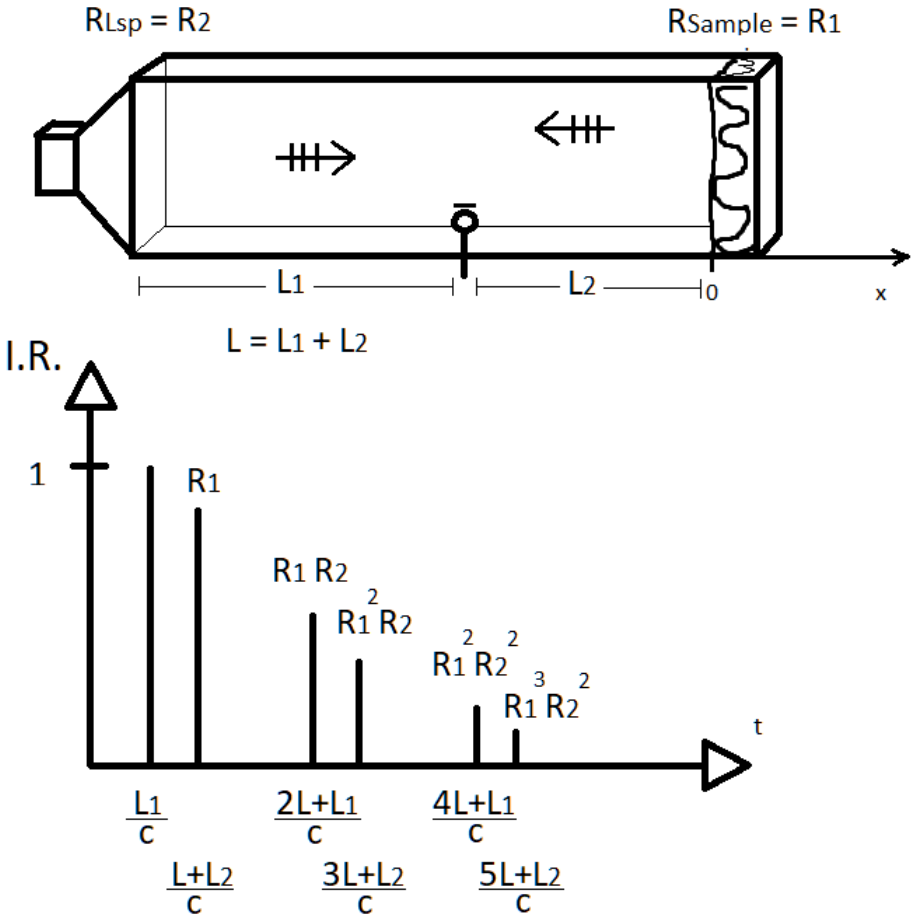

Figure 2.6: Impedance tube & impulse response for Method 3

Method 3 differs from the previously mentioned methods in that it uses reverberation time to determine the reflection factor. It is possible to identify two different sequences from the impulse response pictured in figure 2.6. The first sequence being: $[1, R_1 \cdot R_2, (R_1 \cdot R_2)^2, ...]$, the other being: $[R_1, R_1^2 \cdot R_2, R_1^3 \cdot R_2^2, ...]$. For each sequence, the subsequent pulses will arrive $\frac{2L}{c}$ later, and the amplitude for subsequent pulses will be multiplied by $R_1 \cdot R_2$. The first sequence will be used in this case due to being more simple.
A simplified case of finding $|p(t)|$ is constructed by stating that the first time the sound passes the microphone, the impulse response has a value of 1. After the signal has been reflected once by the sample and once by the loudspeaker, the impulse response will have a value of $|R_{sample} \cdot R_{Lsp}|$. After being reflected a second time by both the sample and the loudspeaker, the value will be $(|R_{sample} \cdot R_{Lsp}|)^2$. Equation 2.22 is constructed for n reflections:

$$|p(t)| = (|R_{sample} \cdot R_{Lsp}|)^n \tag{2.22}$$

This will not be valid for continuous time-values but rather at the instance of t where $t = \frac{2nL}{c}$, c is the speed of sound, and L is the length of the tube.

The equation for the sound pressure amplitude for reverberation time $|p(t)| = Ae^{-\delta t}$ can be used in conjunction with equation 2.22 in order to solve for the combined reflection factor $|R_{sample} \cdot R_{Lsp}|$ using the reverberation time. Where δ gives a reverberation time $\delta = \frac{3ln10}{T_{60}} \Rightarrow T_{60} = \frac{3\ln 10}{\delta}$. Inserting $n = \frac{ct}{2L}$ in 2.22, turns into equation 2.23:

$$(|R_{sample} \cdot R_{Lsp}|)^{\frac{ct}{2L}} = e^{-\frac{3ln10}{T_{60}}t}$$

$$|R_{sample} \cdot R_{Lsp}| = e^{\frac{-6Lln10}{cT_{60}}} \tag{2.23}$$

A single microphone's reverberation time can be calculated from its impulse response and used to get an estimate of the equation in 2.23. The 1D case is discussed in [**7**] and a near identical formula to the first step of 2.23 is shown (for intensity).

One important issue here is that, unlike the previous methods, this Method will yield the reflection factor not only for the sample measured, but the combination of the sample and the loudspeaker. Measurements from a different method like the Method 0, could be used in conjunction with measurements from this method to extract Method 3's R_{Lsp}. By dividing a $R_{sample} \cdot R_{Lsp}$ measurement from Method 3 with a R_{sample} from Method 0, R_Lsp is found, as shown in equation 2.24:

$$|R_{Method3\_Lsp}| = \frac{|R_{Method3\_Lsp} \cdot R_{Method3\_sample}|}{|R_{Method0\_sample}|} \tag{2.24}$$

This division assumes that $R_{Method0\_sample}$ equals $R_{Method3\_sample}$ to find R_{Lsp}, which is not necessarily entirely true. Also, it means that you cannot use this method to find the value for the Method 0 sample used to find R_{Lsp} as it will be exactly equal to Method 0's reflection factor due to the assumption mentioned. This calculated R_{Lsp} can be used to

find the values of other measured samples. Suppose for example, R_{Lsp} is found using the reflection factors where the sample is the empty tube. In that case, this method can be used to find the reflection factor for any other measured sample for Method 3 by simply dividing the measurement with the calculated R_{Lsp}.

2.3.6 The Speed of Sound and Temperature

A simple expression for calculating the speed of sound, c, is shown in equation 2.25 [**8**]:

$$c = 331.4 + 0.6 \cdot \theta \tag{2.25}$$

Here θ is the temperature in centigrade. This formula, however, lacks the effect that humidity has on the speed of sound. A Matlab function "*amb2prop.m*" [**9**] was used instead to calculate c with increased accuracy.

CHAPTER

THREE

EXPERIMENTS

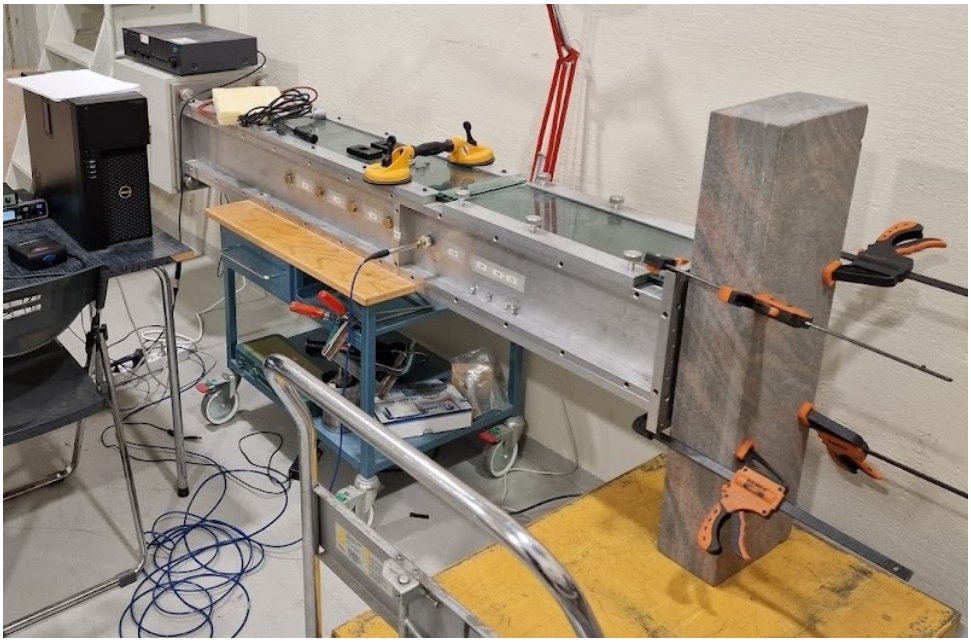

Figure 3.1: Impedance tube measurement

In this chapter, the details surrounding the measurement process will be described. Four different methods being compared. Firstly: The standard two microphone position method, as in ISO 10534-2 [**3**]. Secondly: A five microphone position variation of ISO 10534-2.Thirdly: A five microphone position method using an overdetermined system of equations to solve for the reflection factor using a least mean squares approach. Finally: A reverberation-time based method. A quick overview of this is shown in table 3.1:

Method 0	ISO 10534-2 (2 mic positions)
Method 1	Average reflection factor for 5 mic positions (4 pairs) using Method 0.
Method 2	Least mean squares solution for 5 mic positions using Method 0.
Method 3	Reverberation time method in 1 dimension (5 mic positions)

Table 3.1: The different methods being used.

However, the practical aspect of the measuring process used to acquire the sound pressure data is the same for each method.

A list of equipment used is in a table in appendix A.1. Figure 3.1 illustrates the impedance tube used. It is a square tube with dimensions: Height = 0.2m, Width = 0.2m, and Length = 1.865m. Mic 5 is 0.64m from the wall, and each microphone has a 0.15m spacing between each other. The loudspeaker is a concave half-spherical shape; the length mentioned previously is from the hard wall to the outer edges of the loudspeaker and not to the center of the loudspeaker.

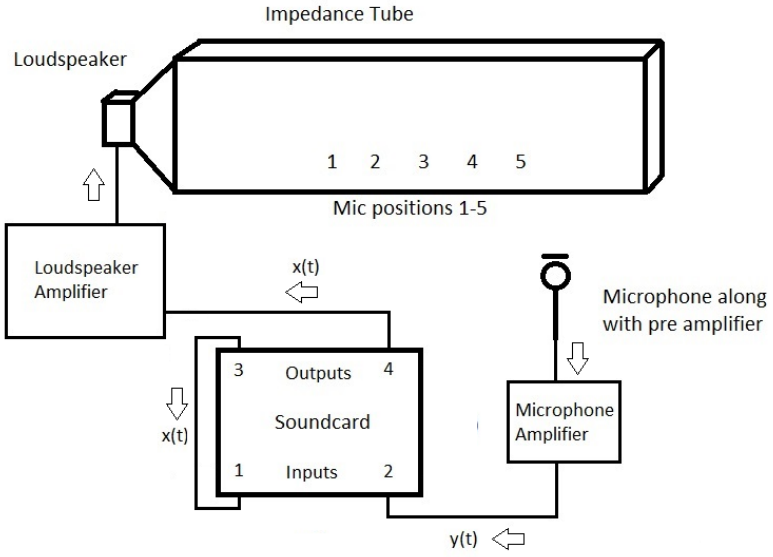

Figure 3.2: 2 channel FFT setup for measurements in impedance tube

The setup shown in figure 3.2 shows the 2-channel FFT setup used during measurements. The output signal $x(t)$ is routed directly into an input to be able to remove the soundcard influence. The output signal is also sent through a loudspeaker amplifier before being sent to the loudspeaker itself and throughout the impedance tube. A microphone can be placed at any of the pre-determined microphone positions and record the signal from the loudspeaker. This signal is then amplified using a microphone amplifier, and this signal $y(t)$, is sent to the soundcard's input. Finally, this data is sent to a sound analyzing software, EASERA, in this case. The output signal used was a logarithmic sweep with pink frequency weighting. Test measurements were performed to make sure there was no clipping and that the signal was sufficiently above the noise floor.

Temperature and humidity were recorded for every microphone during the first measurement set, to see if there were sufficient variations to warrant such frequent measurements of the temperature and humidity. It was decided to only measure the temperature and humidity for measurements performed with microphone position 3. Since the variation in temperature and humidity from the microphone in position 1 to the microphone in position 5 was small, it was decided that such a "median" result for each set would suffice. These temperature and humidity measurements for each set were then used by Matlab function amb2prop.m [**9**] to calculate the speed of sound c for each individual set of sound amplitude measurements.

As the measurements could not all be performed in one day, extra care was taken to ensure the exact same volume amplification on the loudspeaker amplifier. This was done by measuring the voltage over the loudspeaker amplifier to ensure it had not been tampered with and that it was the same at the start of a measurement session. This was done using a 250Hz sine signal.

3.1 Samples used

A low absorbing sample of unknown material, "foam 20mm" is shown along side highly absorbing glass wool sample "glass wool 100mm" in figure 3.3:

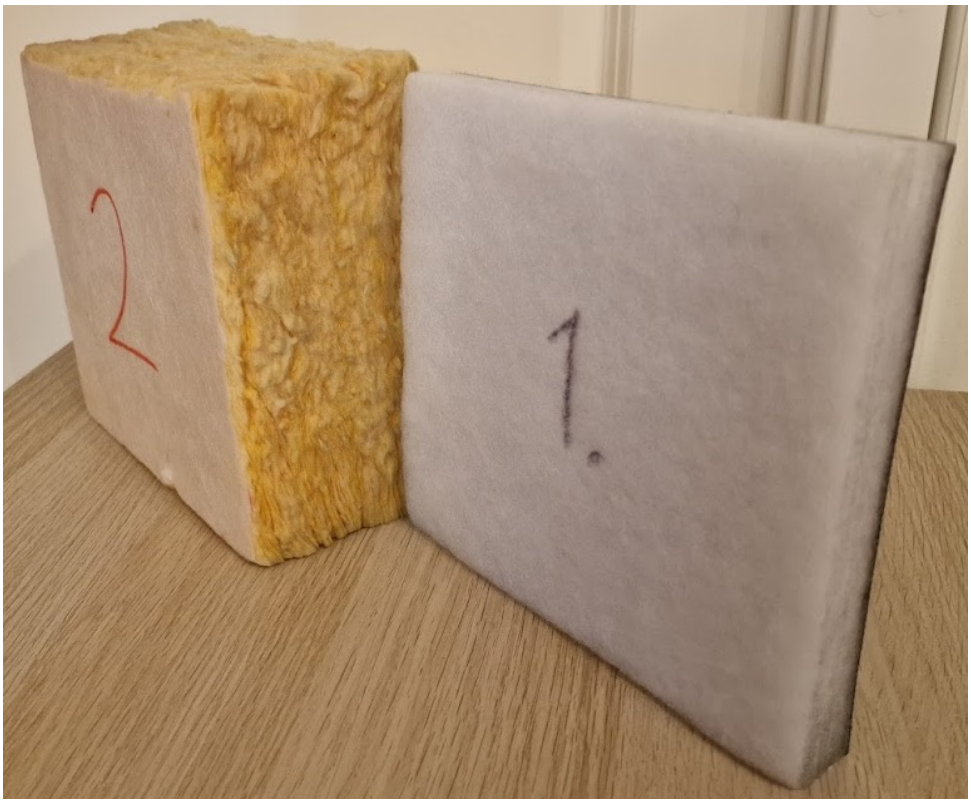

Figure 3.3: Sample "foam 20mm" labeled as 1, and sample "glass wool 100mm" labeled as 2.

Sample "foam 20mm" is 20mm thick, with a somewhat rigid plastic covering on its back. Sample "glass wool 100mm" is a 100mm thick glass wool sample with a rigid white felt-like material on the front and the back.

Sample "rough rock", a large rough stone block is shown in figure 3.4:

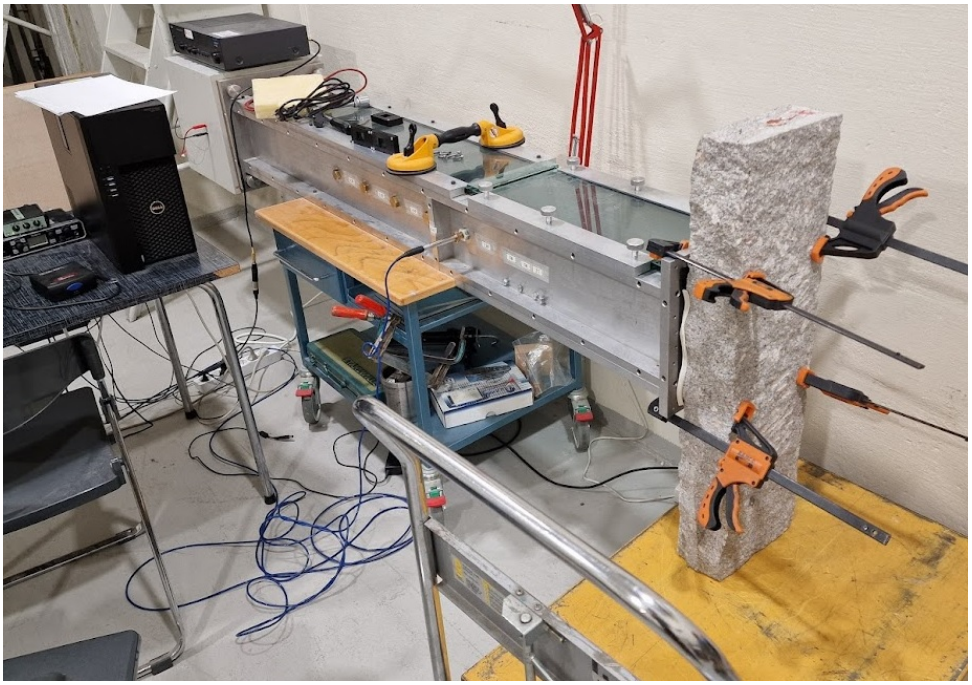

Figure 3.4: Sample "rough rock", a large craggy stone slab.

The sheer size of "rough rock" made it impossible for it to fit within the tube, it also posed a distinctive problem pictured in figure 3.5:

Figure 3.5: Sideview of "rough rock" to showcase unique sealing challenge due to the sample's shape.

Due to the shape of "rough rock", sealing strips of 3.5mm were added to the sample and the tube in a square formation. The area on the sample where sealing strips of the mentioned size could be added and seemed to be enough to seal potential gaps was chosen to be the area under test. There certainly were regions where a sealing strip of that size would not be large enough, which was what was tried to be avoided. However, if there is one sample where an unintentional gap could arise, it would be this sample.

Sample "smooth rock", a large smooth stone block was shown previously at the start of this section but is shown again in figure 3.6:

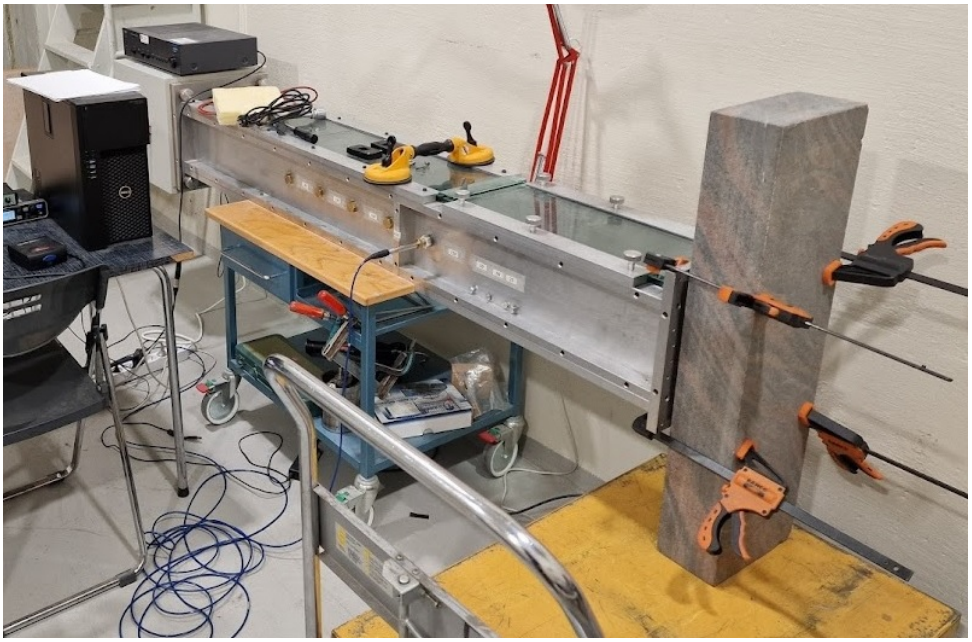

Figure 3.6: Sample "smooth rock", a large polished stone slab

Sample "smooth rock" provides a complete seal over the black gasket at the end of the impedance tube.

Another angle of the measuring situation is shown in 3.7:

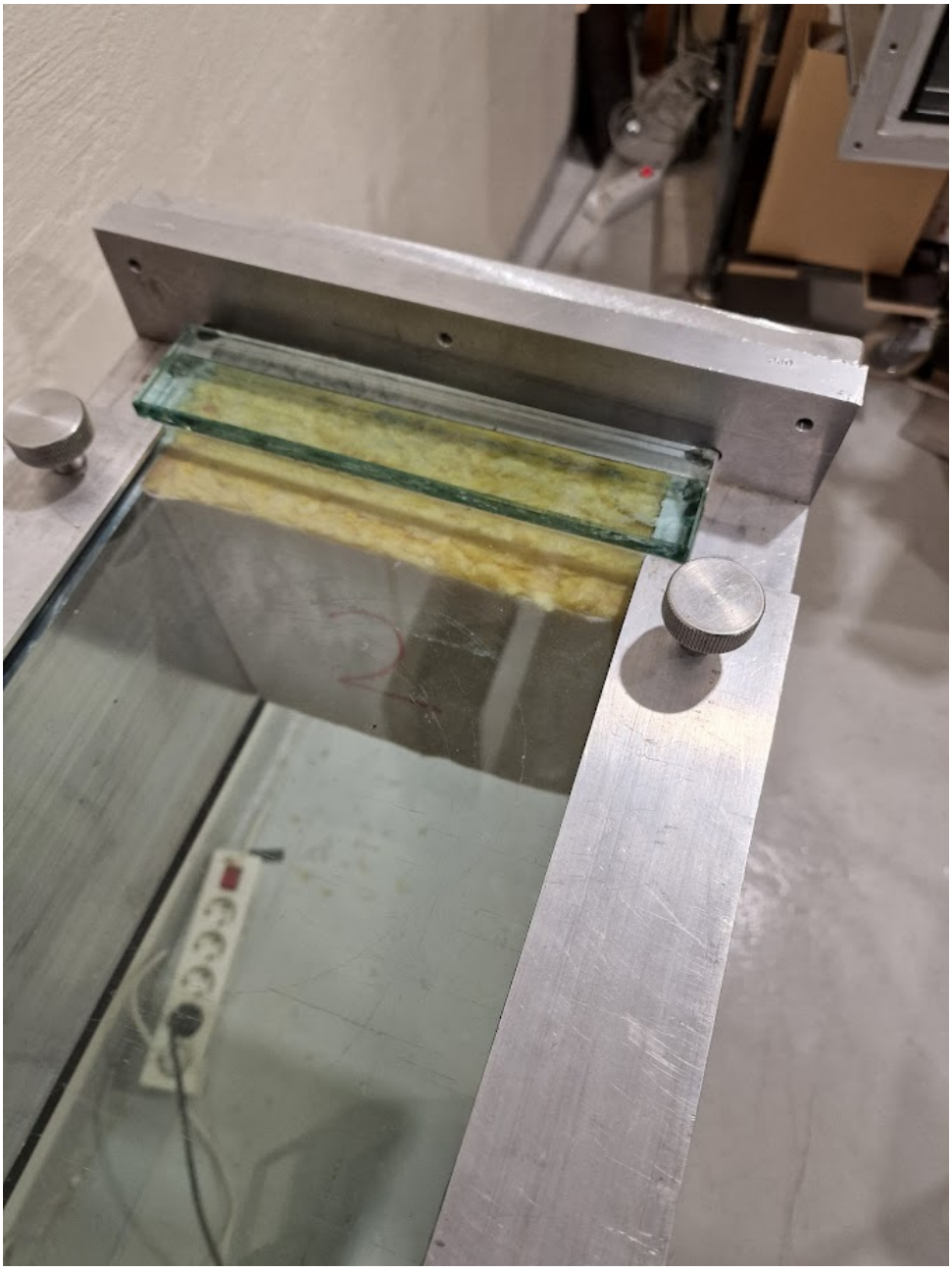

Figure 3.7: Impedance tube measurement with sample "glass wool 100mm"

Here "glass wool 100mm" is snugly fit against the metal covering at the end of the tube, which is secured with 1 screw in each corner. Also pictured are 2 out of 6 knobs that could be unscrewed to remove a portion of the top of the tube for an alternate method to insert the sample (rather than unscrewing the metal covering on the end).

The different samples are compiled in table 3.2:

Sample	Description
"empty"	Sample is the empty tube.
"foam 20mm"	Sample shown in 3.3, length = 20 millimeters
"smooth rock"	Sample shown in 3.1
"rough rock"	Sample shown in 3.4
"glass wool 100mm"	Sample shown in 3.3, length = 100 millimeters

Table 3.2: The different samples being used.

3.2 Processing

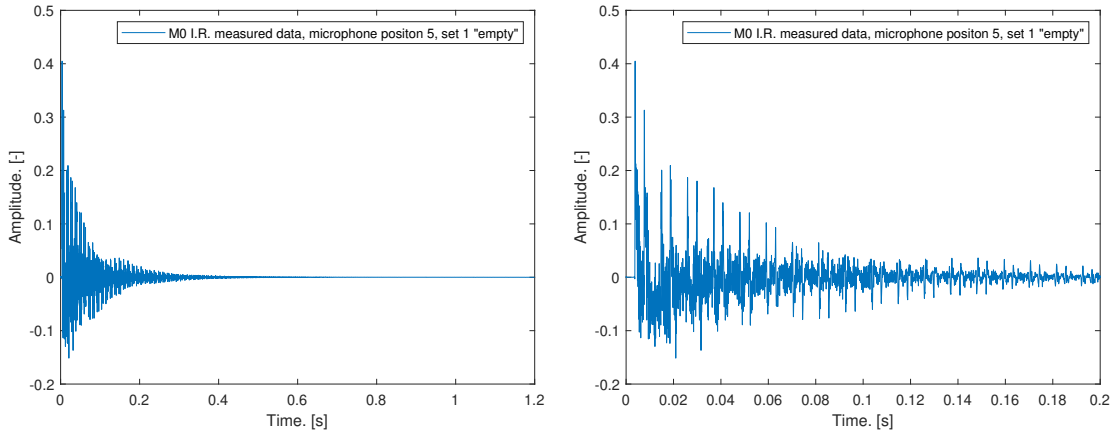

(a) (b)

Figure 3.8: Impulse Response for measured data for microphone in position 5, set 1 of 8. The full used Impulse response shown in (a), and zoomed in for detail in (b), sample "empty"

An example of the impulse response used is shown in figure 3.8. The transfer function $H(\omega)$ was calculated using an FFT of the impulse response $h(t)$ shown in (a). The data used in all FFT calculations for the impulse response was cut at 1.2 seconds to ensure nothing of great importance was removed. In (b) a zoom in on the x-axis of the plot in (a), is shown for increased clarity. Before the FFT was performed, a second order IIR high-pass filter was used at 20Hz. This was done due to some very low frequency noise influencing the impulse response.

CHAPTER

FOUR

RESULTS & DISCUSSION

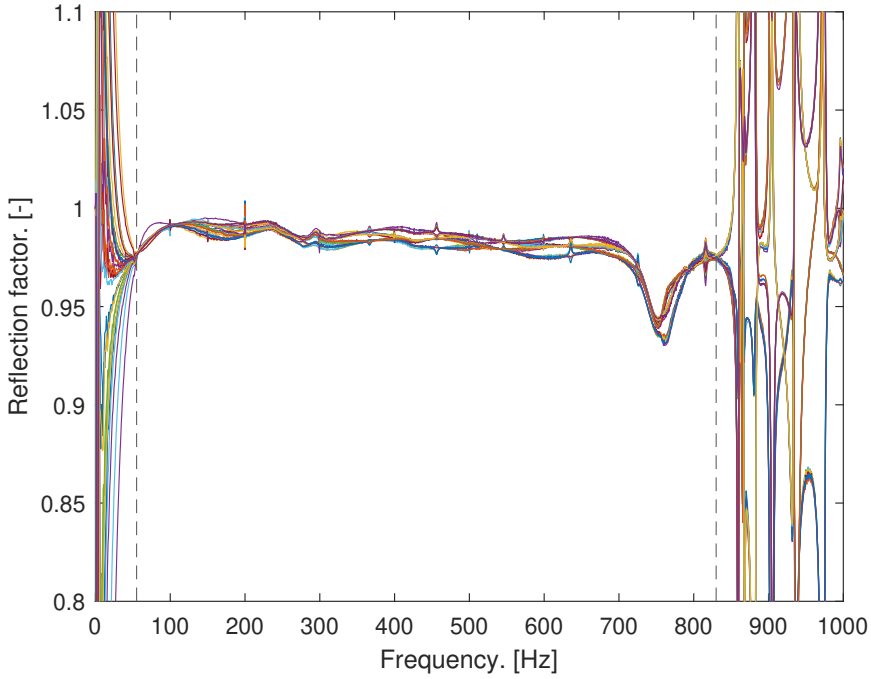

Figure 4.1: The 32 calculated reflection factors for Method 1 using sample "empty"

Figure 4.1 is an example that shows multiple reflection factors using Method 1. As there has been no compensation for propagation attenuation, these curves form distinct groups based on the microphone pair's distance from the wall. Noise also contributes to not seeing four smooth lines here (as there are 4 microphone pairs in Method 1). Two vertical dotted lines have been added to the figure to indicate the lower and upper working frequency range. The lower limit is dependent on the signaling processing equipment used as stated by ISO 10534-2. It was therefore decided through observation to be 55Hz. The upper

frequency limit was calculated using equation 2.15 to be <857.5Hz, and was decided through observation to be set to 830Hz. This was due to what happens to the reflection factors after that point, seen easily to the right of the dotted line at 830Hz.

4.0.1 Unique Attributes of Method 3

A short introductory note to Method 3 is detailed here as it does not share as many similarities as the three other methods do to each other. Methods 0, 1, and 2 use the data from two to five microphone positions, and a high frequency resolution is achieved. Method 3, being a reverberation-time based method, plots reflection factors based on 9 third-octave bands reverberation times calculated by sound analyzing software EASERA. So there will be 9 points versus 1058 for the other Methods. As explained in section 2.3.5, Method 3 calculates a combination of both the reflection factor of the wall/sample as well as the loudspeaker reflection factor. To compare Method 3 to the others, samples measured using Method 3 were divided by empty tube measurements using Method 3. This should remove the influence of the loudspeaker reflection factor, but leaves you with a reflection factor divided by a reflection factor relationship. This relationship between "reflection factor of the sample divided by reflection factor of the empty tube" is compared to the same relationship for all other Methods in figure 4.2, to check the validity of results in a comparable manner.

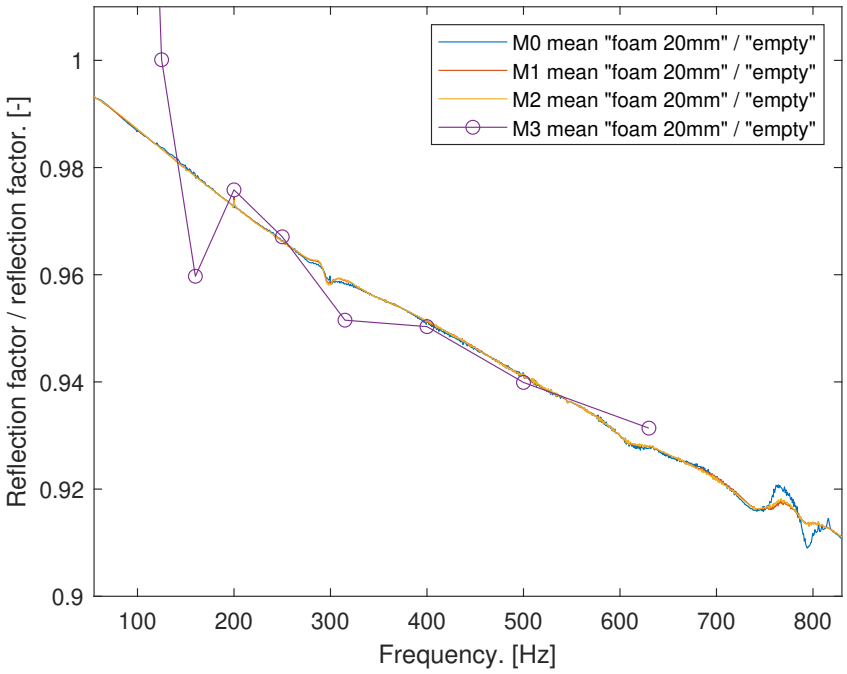

Figure 4.2: Reflection factor mean values for a sample divided by the empty tube for all methods, sample "foam 20mm" divided by "empty"

In figure 4.2, the relationship of the reflection factors for "foam 20mm" divided by "empty" is shown. All other samples behaved similarly to the one depicted, where the first two to three results for below 200 Hz, deviate noticeably compared to the other Methods.

The following results, however, seem to follow along with Methods 0, 1, and 2 relatively well. This means that the first few results shown for the lower third-octave bands are likely wrong. Method 3 is the only method where only one microphone is required, as the reflection factor is calculated using reverberation times. However, if no other method is used to find and remove the influence of R_{Lsp}, one will be stuck with either results in the same form as in figure 4.2 or the reflection factor combined with R_{Lsp}.

The reflection factor for the loudspeaker was calculated as described in 2.24 and shown in figure 4.3.

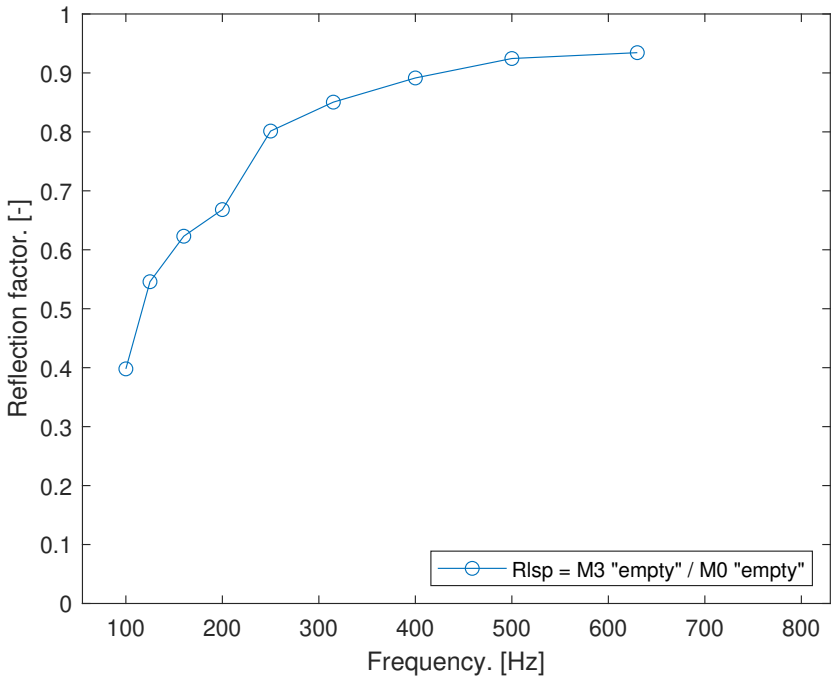

Figure 4.3: Reflection factor for the loudspeaker R_{Lsp} calculated Using Method 3's reflection factor of the empty tube divided by Method 0's reflection factor for the empty tube, sample "empty"

Even though the reflection factor for the loudspeaker is apparently quite a bit lower at lower frequencies, it does not influence the ISO Method 0, and by effect, Methods 1 and 2 as well. This does, however, impact the reflection factor for a measured sample by a large amount, and shows the need to eliminate R_{Lsp} to achieve correct results for Method 3. Method 3 will consequently rely on using a second method. If one uses Method 0, which uses two microphone positions, and performs a set of measurements for the empty tube, single microphone measurements from Method 3 will then be enough for subsequent measurements of samples. This can be seen as a potential advantage this method has over the others. Another minor advantage this method has, is that many measurement instruments implement the measurement of the reverberation time, which is what this method needs

The importance of compensating for propagation attenuation will be seen in the following

sections. Unfortunately, it was unclear how this would be done for Method 3 and is therefore not present in compensated results shown later on.

4.1 Reflection Factors Without Compensation For Propagation Attenuation

Figure 4.4 show the mean values of the uncompensated reflection coefficient for each of the 4 microphone pairs, 1-2, 2-3, 3-4, and 4-5 calculated using Method 0 (compare this to the introductory figure 4.1):

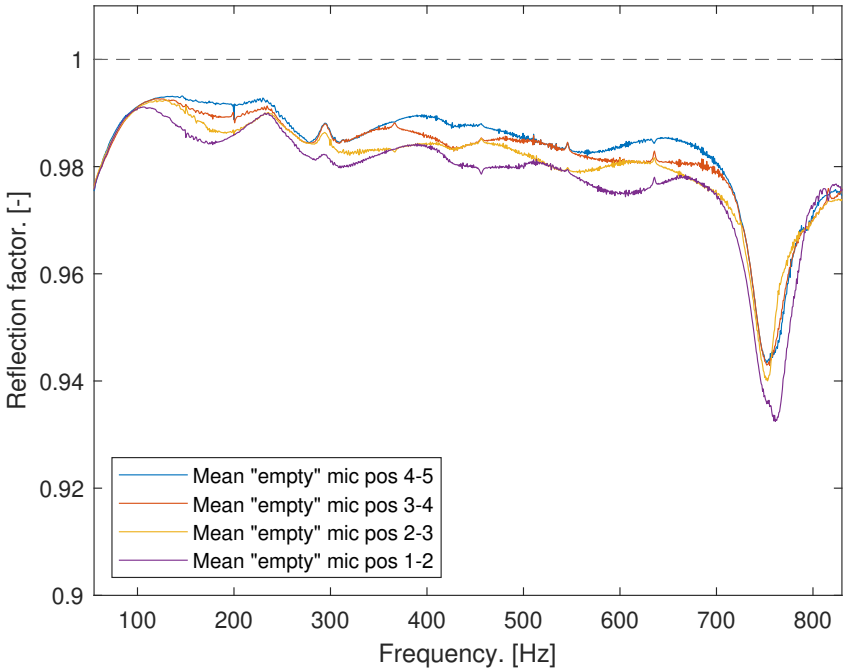

Figure 4.4: Reflection factor mean values for each microphone pair, sample "empty" Method 0

This graph in figure 4.4 makes it clear there is a definite difference in the measured reflection factor based on the distance the microphone pair is placed away from the sample/wall. It also shows a problem that will arise for Methods 1 and 2, when not taking sound attenuation into account. While Method 0 uses the closest microphone pair, and hence achieves the highest reflection factor, Methods 1 and 2 both use a combination of all four microphone pair's reflection factors. This causes them to have lower reflection factors in comparison. The dip, which is clearly visible in the 700-800Hz range, was considered to be the result of some unknown leakage. This will be discussed in a later section.

Figure 4.5 shows all methods with their calculated reflection factors for the polished stone slab sample "smooth rock":

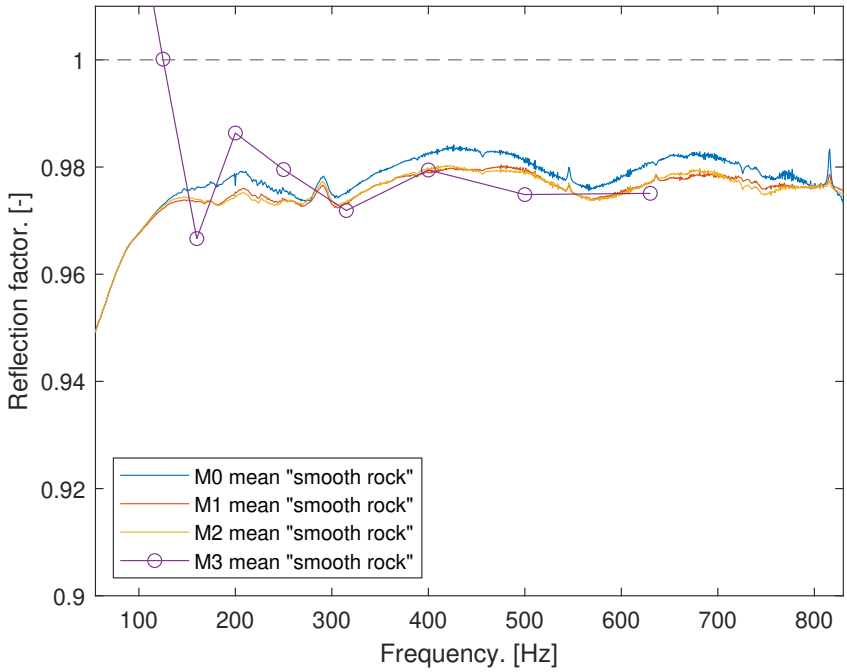

Figure 4.5: Reflection factors for all methods without any compensation for propagation attenuation, sample "smooth rock"

Because Method 1 is an average of 5 microphone positions and Method 2 is the least mean squares solution, these two methods are expected to display similar results. Both methods use microphones further away from the sample, which should lead to a lower reflection factor. This can indeed be seen in figure 4.5, with Method 0 having the highest reflection factor. This is because it is based solely on the microphone pair closest to the sample. Hence there will be less distance for the sound wave to be attenuated by. Method 3 shows a a surprising disparity compared to other Methods, for the lower frequency bands, before settling alongside the other Methods relatively closely. The next third-octave band above 630Hz had to be removed because the band included frequencies above the upper limit. It was thought then that perhaps that is the reason for the poor first result at least, for Method 3, but the 100Hz third-octave band was well above the allowed frequency range set (>55Hz).
The dip in the 700-800Hz range seen in figure 4.4 is not present in figure 4.5. This leads one to believe that there is no problem with leaks for "smooth rock". It is mentioned in [**10**], that humidity has an effect on sound reverberation measurements and sound attenuation. It suggested a method that reverberation time measurements can be corrected to a similar humidity and temperature to eliminate discrepancies stemming from differences in temperature and humidity between measurements. The temperature stayed between 18.64-19.71 centigrade for all measurements, and on average 32% humidity for the two stone samples, and 38% on average for the rest of the samples and the empty tube. The effect of differences in humidity, as can be seen in figures of [**10**], became much more substantial at higher frequencies (>1000Hz) and much less so for the lower frequency bands in question here (in the temperature range described). For this reason, the correction was

not performed.

Figure 4.6 shows all methods with their calculated reflection factors for the highly absorbing glass wool sample "glass wool 100mm":

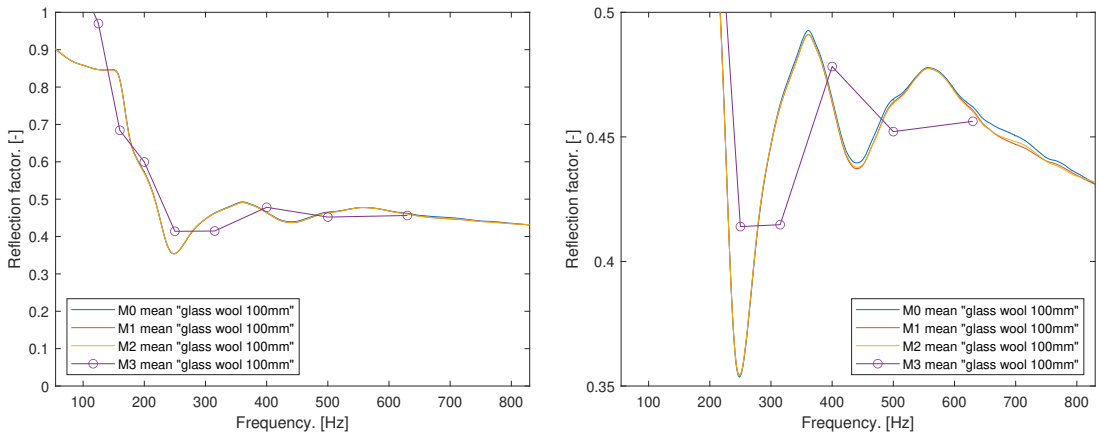

Figure 4.6: Reflection factors for all methods without any compensation for propagation attenuation, sample "glass wool 100mm" in (a) zoomed in y-axis in (b)

The y-axis is extended to get a full view in figure 4.6 (a), and zoomed in to view more details in (b). There really is very little difference at all between methods 0, 1, and 2, which this figure should make clear. Method 3, similarly to as seen in figure 4.5 for "smooth rock", once again has seemingly wrong results for the two lowest frequency bands.

None of the reflection factor measurements as seen in figure 4.6 or in figure 4.5 (or for all results not shown) satisfy the requirement set by ISO 10534-2 for the maximum distance away from the sample/wall [**3**]. As mentioned in section 2.3.2, if the microphone closest to the sample is over three maximum lateral dimensions away, compensation for propagation attenuation must be performed.

4.2 Influence of Compensating for Sound Attenuation

Microphone pair 4-5, which was used by Method 0 to determine the reflection factor, is 0.64 meters away from the sample "smooth rock" in the previous figure 4.5, and the maximum length it could be without needing compensating according to the ISO, is in this case 0.60m. Sample "smooth rock" just barely requiring compensation. At the same time, due to sample "glass wool 100mm"'s 100mm extra length comparatively, the distance between microphone and sample becomes 0.54, not requiring compensation. However, all samples will be compensated for attenuation loss for the entire way to the sample/wall.

The data shown in this section was obtained using the extra microphone positions beyond what Method 0 requires. Microphone pairs at different distances from the sample/wall

are tested. One thing to keep in mind is that if one wants to compensate Method 0 experimentally this way, 4 microphone positions are needed. At that point, Method 1 or Method 2 using 4 microphone positions would technically not have the downside of needing additional microphone positions compared to Method 0.
Compensating for attenuation in the following results was done as described in 2.10. It was initially assumed that this could be done once and would function well for describing loss from attenuation for the tube. Having done this for the empty tube , seen in figure 4.7 and for other samples (not pictured), quickly revealed that k" found for one sample, will not work well in conjunction with other samples. One individual k" would be needed for each sample. However, this comparison is not shown.

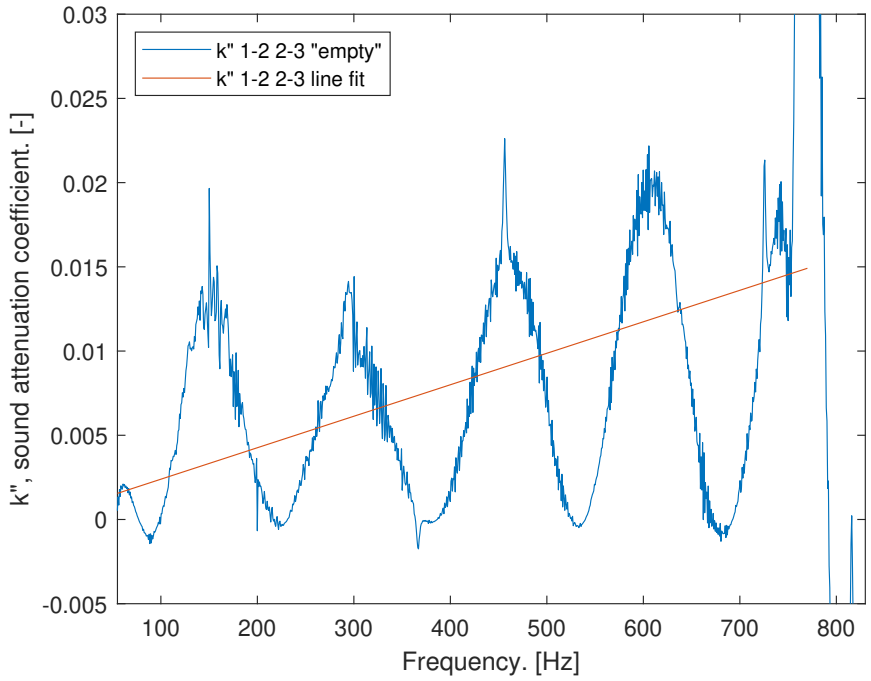

Figure 4.7: Sound attenuation factor from microphone pairs that share common microphone in position "2", for the empty tube.

In figure 4.7, it is possible to see that when one attempts to determine the sound attenuation using a microphone directly next to each other such as 1-2 and 2-3, the sound attenuation appears to oscillate rather than remain at a somewhat stable value. It even reaches 0 several times, implying that certain frequencies do not attenuate, which should not be happening in reality. This oscillation seems to depend on the distance the two pairs are from the sample/wall, and the frequency of oscillation increases the further the pairs are from the sample/wall. In appendix A.1, plots of k" for microphone pairs 2-3 & 3-4 or 3-4 & 4-5 show this relationship. So there might be a way to account for the oscillation if it can be predicted with a formula devised through results such as these. However, it was decided to use a line-fit for k" to lessen the impact of the oscillating effect.
A line-fit for k" (attenuation constant), assuming the form $a \cdot f + b$, was made based on the data from the 55-770Hz range. The simple line-fit shows that the attenuation trend at least is happening according to the expectation that the attenuation is slowly increasing

as the frequency increases.
If a high degree of accuracy is desired, one could be making unintentional mistakes by somehow not taking this oscillating effect into consideration. Although with that said, it is not a phenomenon that was completely understood. The phenomenon has been credited to possibly be some artifact from the signal processing equipment used, or of the calculation method for the reflection factors. This type of issue could be more troublesome when using Method 0. This is as the user may never be aware of it being there since there is no other microphone pair position to compare reflection factors to and notice that the problem even exists.

Figure 4.8 shows the attenuation constant that was determined using microphone pairs that are further away from each other and do not share a common microphone:

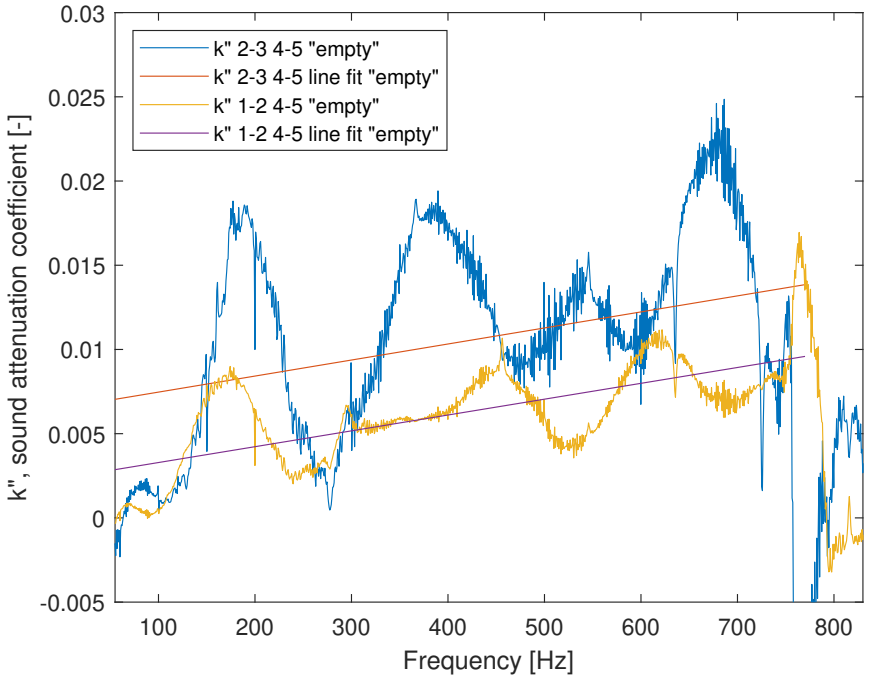

Figure 4.8: Sound attenuation factor from microphone pairs that do not share a common microphone for the empty tube.

In this case, the result seems more convincing, as in both cases, the attenuation does not reach 0 (except in the extreme ends) as it did in figure 4.7. Higher frequencies are expected to attenuate more quickly than lower frequencies, which shows in this plot where the attenuation factor rises slowly with frequency. The oscillation effect does remain, however and again, it can be seen that the frequency of oscillation is different for both the 1-2 & 4-5 pairs and the 2-3 & 4-5 pairs. Another interesting observation is that the k" values determined using 2-3 & 4-5 pairs seem to be noticeably larger than 1-2 & 4-5. Perhaps there is a higher concentration of sample remnants from previous use of the impedance tube in the area that is closer to the sample insertion side. Some tiny specks of wood particles were observed in the tube (while most particles were removed, there was

no thorough cleaning performed on the tube).
As it was thought that the furthest distance between microphone pairs would give the best and most representative value for k_0'', the 1-2 & 4-5 pairs were decided to be used in all cases of compensating for propagation attenuation. This is also the reason behind the choice of 55-770Hz for the line-fit, as there is a sudden change in the behavior of the curve after 770Hz for the 1-2 & 4-5 pair. This is most likely due to the fact that there is an interesting dip in the reflection factor in this area.
It must be stressed, however, that this oscillating effect will cause some erroneous results. Using k_0'' determined from the 1-2 & 4-5 microphone pairs to see the reflection factor of 1-2 as if it were in the 4-5 spot will work perfectly. However, using that same k_0'' factor on 1-2 to see what it would look like in the 2-3 spot for example, will show a slight variation if compared with the actual measured reflection factor from 2-3. This is show in figure 4.9:

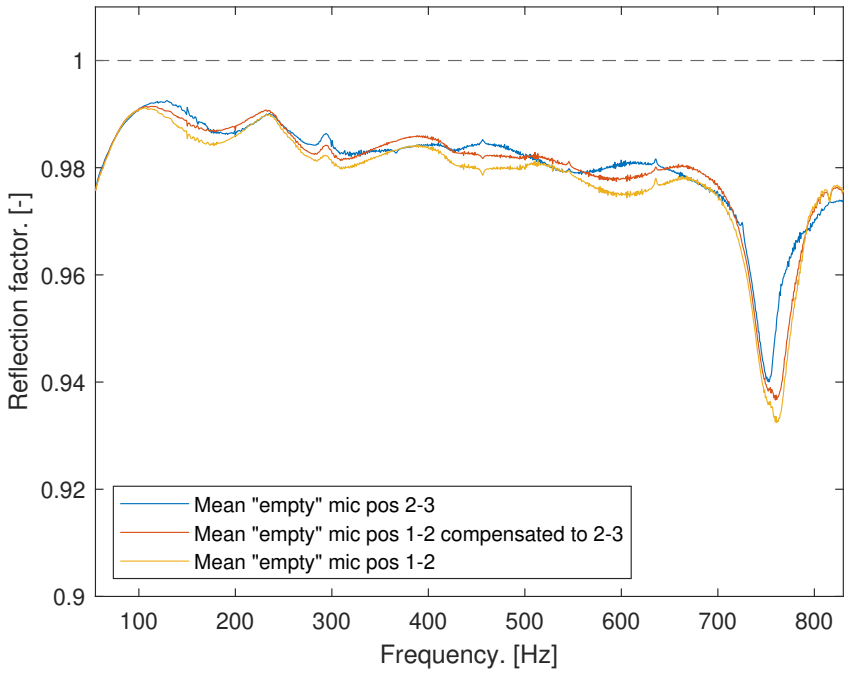

Figure 4.9: Measured reflection factor compared to compensated, using oscillating k" value, sample "empty"

Results from figure 4.9 show that the attenuation factor can not be used to perfectly recreate 2-3 from 1-2 as the compensated value hovers mainly between the two measured pairs. The process of compensating for propagation attenuation will be imperfect, but methods 1 and 2 will always be at a disadvantage without it being performed.

4.3 Reflection Factors Compensated for Sound Attenuation

The following results are the reflection factors, attenuation compensated as described in section 2.2, for Methods 0, 1, and 2. Method 3 is not included as it is unclear how

compensation would be performed.
Even though section 4.2 showed that performing compensation for propagation loss indeed has its issues, it would be very interesting to see reflection values potentially closer to the true value. This is done by compensating for sound attenuation all the way until the sample/wall. As it is not possible to simply measure next to the sample/wall due to non-plane wave propagation, this compensation must be done instead. Figure 4.10 shows the compensated reflection factors for Methods 0, 1, and 2:

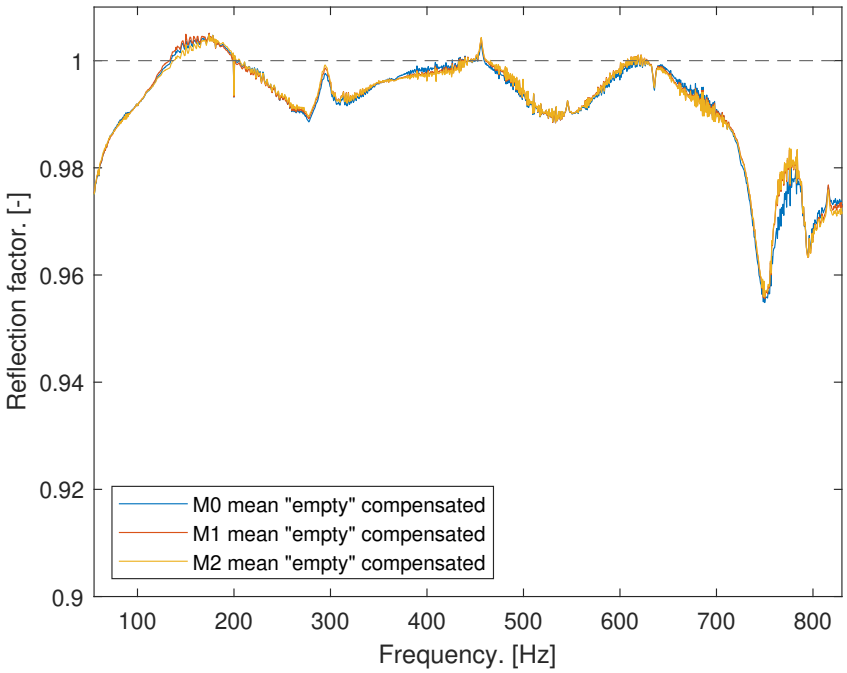

Figure 4.10: Compensated reflection factors for methods 0, 1, and 2, using oscillating k" value, sample "empty"

It can be seen in figure 4.10, that all 3 methods shown after compensating for propagation attenuation have a very high degree of overlap, to the point that it is difficult to distinguish between them other than Method 0's slight divergence around 770Hz. Unfortunately, at 150Hz, there is an obvious unrealistic occurrence where for some nearby frequencies, the reflection factor reaches beyond the max of 1. This is, of course, not possible in real life, and the reason it happens is most likely due to a peak in k" at certain frequencies (notice what happens to 'k" 1-2 4-5' in figure 4.11 for 150Hz). Compensating for propagation attenuation over long distances exacerbates the issue of the peaks and valleys of k". For this reason, the line-fit for k" was deemed a more appropriate choice.

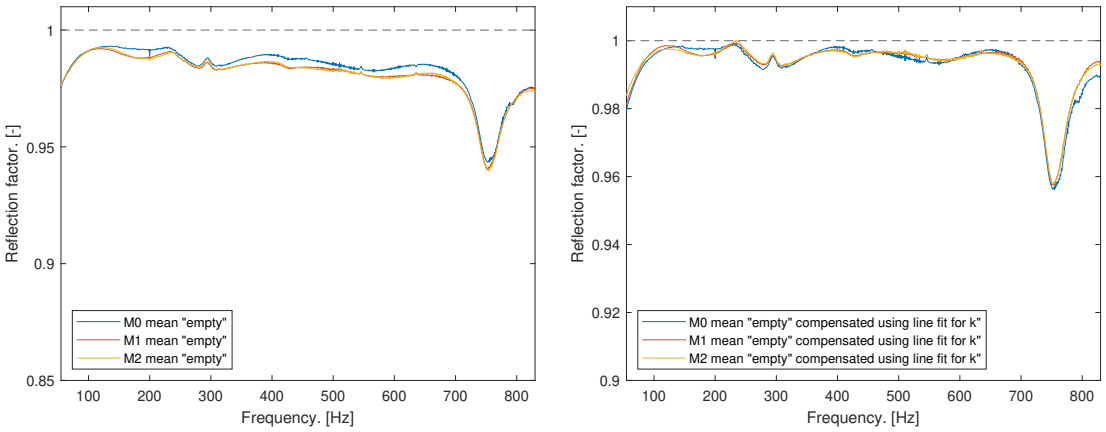

(a) (b)

Figure 4.11: Reflection factor without line-fit propagation attenuation compensation in (a), and with, in (b), sample "empty"

Other than a suspicious dip in the reflection factor in figure 4.11, occurring between 700 and 800Hz, this seems like a reasonable result for the metal covering used as the hard wall for the impedance tube. The dip is suspected of being leakage in the tube and is discussed in a later section. It does seem to be centered around the metal covering one way or another, as the low absorbing sample "foam 20mm" also experiences this dip, while both of the rock samples, that do not use the metal covering, don't. The sample "glass wool 100mm" does not show this dip either but it is a highly absorbing sample and that could easily be the reason why it is not seen.

Figure 4.12 shows theses 3 methods again for the highly absorbing glass wool sample:

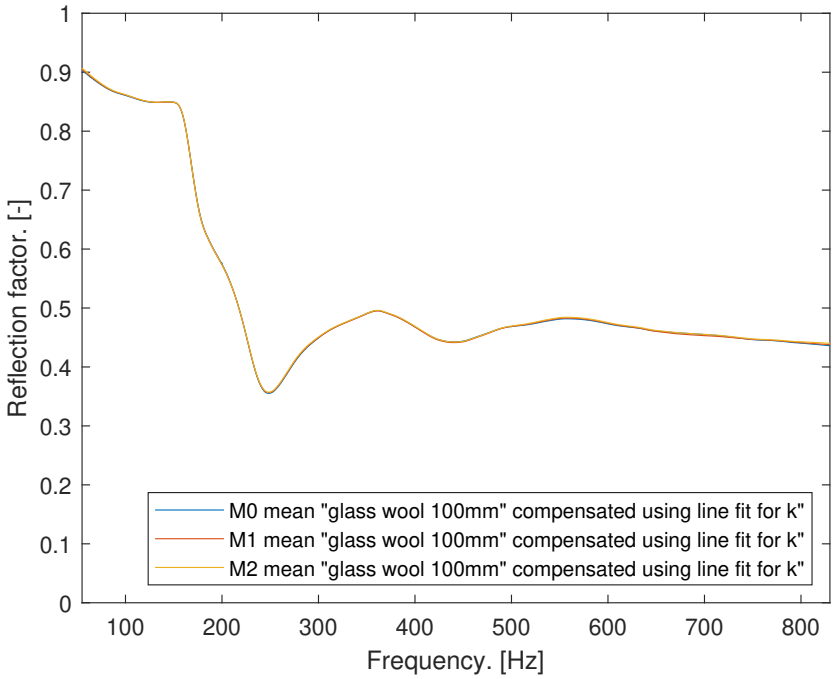

Figure 4.12: Compensated reflection factors for methods 0, 1, and 2, sample "glass wool 100mm"

The y-axis is extended again for the glass wool sample in figure 4.12. Variations are slight, and it becomes evident that no single method can be deemed better than another in this way as they are simply too similar. Perhaps other metrics can be useful in deciding whether one Method is better than another.

4.4 Statistical Analysis

First, one important thing regarding the measurements of the samples. It was initially the intent to remove a sample and reinsert it between each set. However due to the difficulty concerning moving the enormous and heavy rock samples, it was decided that they should remain stationary for all sets. Out of fairness to the other samples it was decided to redo measurements for the other samples without removing end reinserting between sets. The variance in results will certainly be lower due to this.

As Methods 0, 1, and 2 in particular share very similar results, one method could possibly be shown as having a lower variance and can therefore be deemed to be better in that aspect. To visualize differences in variances from the reflection factor results, error bar plots with 95% confidence interval were planned to be made.

It is important to achieve an as fair as possible comparison between methods. Even though Methods 0, 1, and 2 are quite similar, the difference in the error could be nearly twice as big just from a change of definition. In Method 1, for instance, there are 32 measure-

ments, 8 from 4 different microphone positions each. While this would give an advantage of being >30 measurements, allowing using z-value rather than 'Student's t' t-value for calculating the confidence interval, a problem showed itself. When comparing the method 1 mean values of the reflection factors in figure 4.4, it is easy to see that Method 0 will outperform Method 1 with a lower variance. As Method 0 is simply 1 of those means, while Method 1 is going to have a much larger variance due to how distinctly different those reflection factors from different microphone positions are. This is the fault of the sound attenuation that the differences in microphone positions lead to. As was seen in figure 4.9, compensating for sound attenuation was not a perfect fix. Therefore, none of the confidence intervals were created using compensated values as it would just introduce more errors. However, to be more fair to Method 1 in comparison to Method 0 and Method 2, it was decided to, instead of calling n = 32 measurements, to say that n = 8 means (of 4 reflection factors for the 4 pairs which comprise 1 set). This way, the variance is between each of the 8 measured sets for method 1. This makes it much more comparable to, for instance, Method 2, whose least mean squares solution best fit could be viewed akin to a mean.

These 95% confidence interval error bar plots, however, due to the sheer amount of data points, could not convey the desired information in a legible manner. Therefore the following figures are simply plots of the margin of error for the 95% confidence interval multiplied by the appropriate distribution value rather than showing thousands of error bars. Since it was decided in the previous paragraph that n = 8 for all Methods, the distribution will be a student-t distribution and the appropriate value for the 95% confidence value is $t_{value} = 2.365$, which is multiplied with the standard error and is called, the margin of error $(t_{value} \cdot \frac{\sigma}{\sqrt{(n)}})$.

Figure 4.13 shows the margin of error of the reflection factor calculated for all Methods for sample "empty" and "smooth rock".

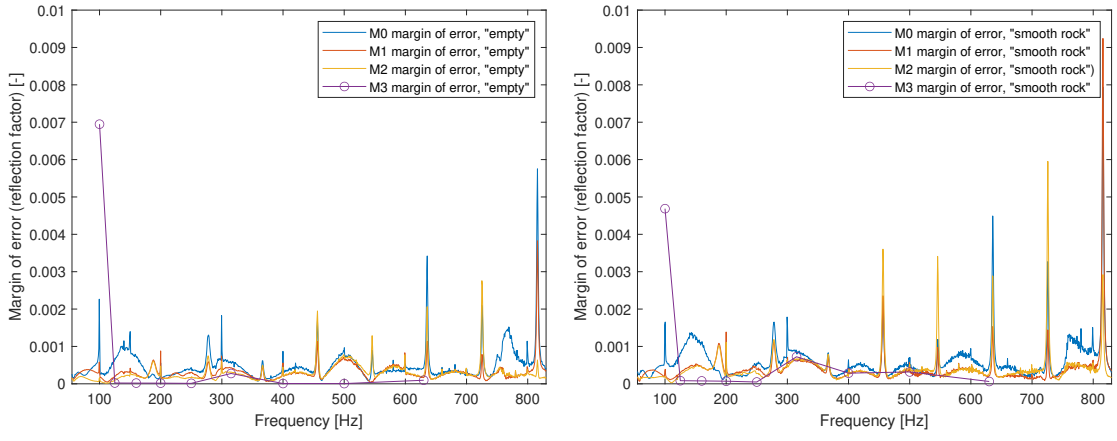

(a) (b)

Figure 4.13: Margin of error for the reflection factor, 95% confidence interval, sample "empty" in (a) and sample "smooth rock" in (b)

First off, figure 4.13 (b) was included as it best shows off a possibly tube-related phenomenon throughout many of the results. This is also easily visible in the non-mean introductory figure 4.1. A periodic effect occurs about every 88-90Hz when measuring the peaks. Exactly what is the cause is uncertain, but it is present in all measured data.

Figure 4.14 shows the margin of error of the reflection factor calculated for all Methods, for sample "glass wool 100mm"

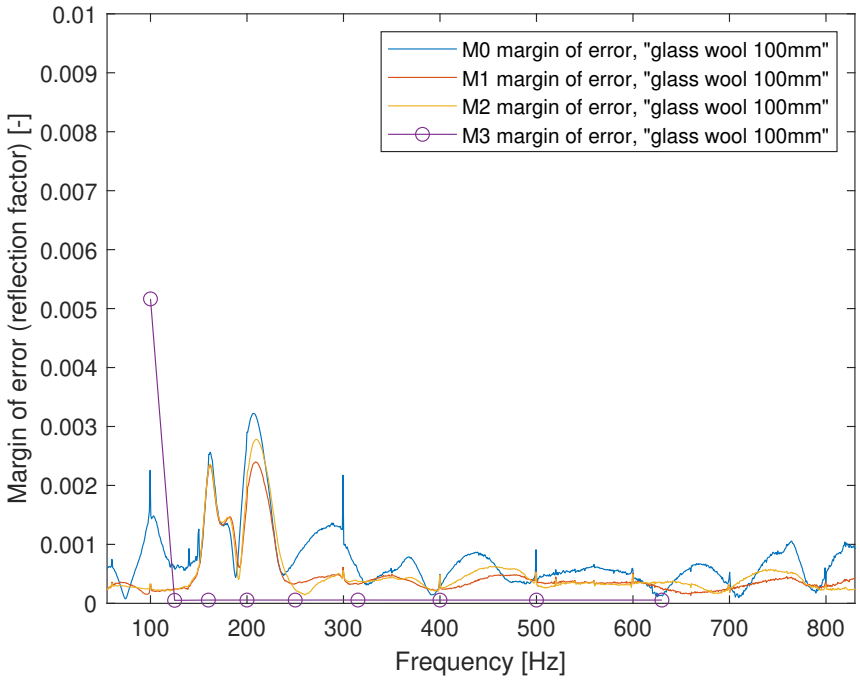

Figure 4.14: Margin of error for the reflection factor, 95% confidence interval, sample "glass wool 100mm"

As has probably become apparent after viewing these margin of error plots, Method 3 is behaving rather oddly once again. The margin of error seems to be very low compared to the other Methods. This is believed to be due to the sound analyzing software used, EASERA. EASERA calculates reverberation times up to T_{30}, this extrapolated value is used as a substitute for T_{60}. Unfortunately, the number of decimals provided for the T_{30} values by EASERA was capped at two. This resulted in very similar T_{30} values most of the time. This limit on decimals provided introduces a bias error. Due to the random variations being lower than this introduced error, the margin of error appears to be 0 for some bands. The effect of this rounding error could have been calculated but was not done here. This could also account for some of the differences between Method 3's calculated reflection factor and the other Methods' reflection factors.

The sum of the margin of error for each Method other than Method 3 (not included due to the previously mentioned oddities) was divided by the number of data points within the 55-830Hz range. This way, the average margin of error for Methods 0, 1, and 2 could

be compared to see if one Method would stand out. It was decided to do this for the most reflective sample, "empty", and the most absorbing sample, "glass wool 100mm", to see if this would impact the average margin of error for a Method.

Table 4.1: Average margin of error for calculated reflection factors.

Sample	**Method 0**	**Method 1**	**Method 2**
"empty"	$4.88 \cdot 10^{-4}$	$3.08 \cdot 10^{-4}$	$2.87 \cdot 10^{-4}$
"glass wool 100mm"	$7.45 \cdot 10^{-4}$	$4.71 \cdot 10^{-4}$	$5.09 \cdot 10^{-4}$

It can be seen in 4.1 that Method 0 in both the case for the sample "empty" and "glass wool 100mm" has the greatest margin of error. Method 0 has a 70% larger error than Method 2 (the lowest) for sample "empty". Method 0 also has a 58% larger error than Method 1 (the lowest) for sample "glass wool 100mm". Method 1 and 2 have a similar margin of error to each other for each sample, but neither Method 1 nor 2 has the lowest margin of error for both samples.
While Method 0 uses data from 8 sets multiplied by 2 mic positions = 16 microphone measurements, Methods 1 and 2 both use 8 sets multiplied by 5 mic positions = 40 microphone measurements. This might have become more favorable for Method 0 if 40 microphone measurements were used instead of 16. However, at the same time, there is no compensation done in these margin of error results to account for sound attenuation. This gives Method 0 a significant advantage compared to Methods 1 and 2.
One final thing of note is that Method 1, using 4 microphone pairs, ends up using microphone 2, 3, and 4, twice per set which could contribute favorably for Method 1 compared to Method 2, which uses all microphones 1 time only per set.

4.5 Absorption Coefficient α

In this section, the absorption coefficient, α, will be shown for the most reflective sample, "empty", and for the most absorbing sample, "glass wool 100mm". The potential error that can be made when calculating α without compensating for propagation attenuation will be shown for both samples using Method 0. Compensated Method 1 α results will be compared against Method 0, and compensated Method 2 results will also be compared against Method 0. One α plot will be shown for Method 3, but it will not be compared to Method 0 due to Method 3 as there are no uncompensated Method 3 results for "empty" as mentioned at the end of section 2.3.5 and there are no compensated results, as mentioned in section 4.3.

Figure 4.15 shows values for the absorption coefficient for sample "empty", calculated with an uncompensated reflection factor and one calculated using a reflection factor compensated using a line-fit for k":

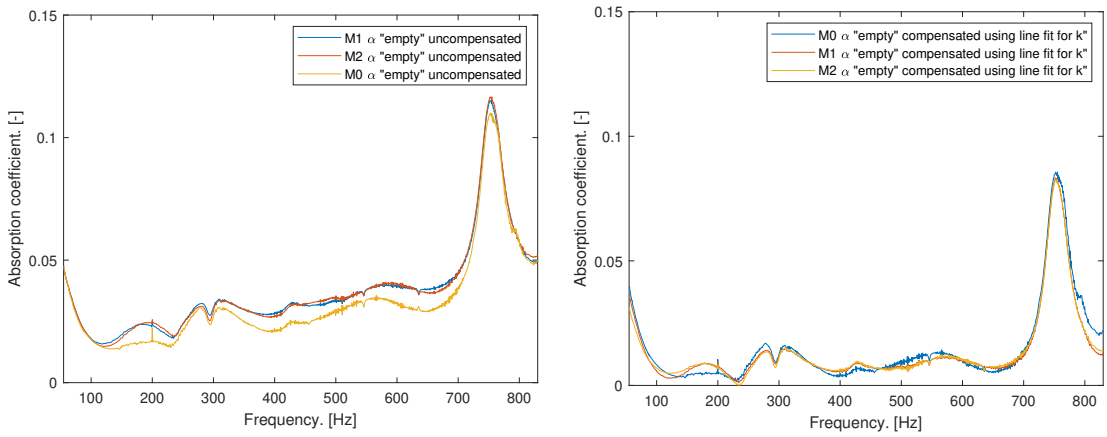

(a) (b)

Figure 4.15: Absorption coefficient calculated without compensating for propagation attenuation in (a) and calculated using compensated reflection factor in (b) for Method 0, 1, and 2, sample "empty".

Be aware that the y-axis here is different in these plots for α in 4.15. One can see a large difference between the uncompensated and compensated results in (a) and (b), respectively. There is also, however, a noticeable difference between the compensated results between Method 0 & Method 1, and Method 0 & 2, which will be discussed first. How much difference is there between Method 0 and 1, or between Method 0 and 2? As Method 0 is not strictly only above or only below the other Methods as seen in (b), it was decided to calculate the absolute value of the difference between the two Methods for both cases mentioned. Using this value, it was shown that Method 0 is, on average (over the entire 55-830Hz range shown) 14.9% different from Method 0 (relative difference). In the same way, Method 0 was calculated to be, on average 16.3% different from method 2 (relative difference). Throughout this paper, Method 0 has been assumed to be the most correct; Method 0 is also being used to determine the value for Method 3 without R_{Lsp}. Suppose one imagines that Method 2 is actually the best and near 100% correct, then there is a noticeable 16.3% difference when calculating the absorption coefficient, (14.9% in the case of Method 1) if one uses Method 0. A decently sized error could potentially be made. Of course, one can not simply say that Method 1 or 2 is the better Method; it could just as easily be Method 0 still that is the more correct. Though it is possible to see in (b) that the smoothness from Method 1 and 2 lessens the impact of spikes and other effects caused by the position of the microphone pair in the results as compared to Method 0.
When the same calculations were performed for "glass wool 100mm", the difference in Methods 1 and 2 compared to Method 0 was much lower. Method 1 absorption coefficient results were only 0.13%, different and Method 2 was 0.18% different from Method 0 for this high absorption sample (relative difference). Again, if Method 1 or 2 then are the most correct Methods, then there is mainly only a large impact on the results if the samples being measured are highly reflective.

Figure 4.16 shows the uncompensated results for all methods:

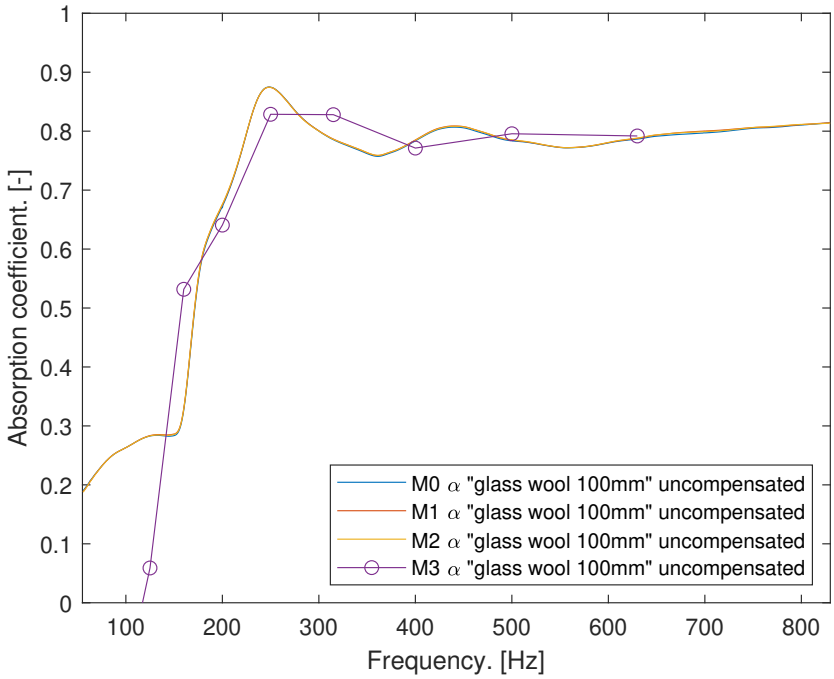

Figure 4.16: Absorption coefficient calculated without propagation attenuation compensation for all methods, sample "glass wool 100mm".

As seen in the results for the reflection factor regarding Method 3, the first two to three results seem a bit off. It then appears to stabilize and follow the other methods somewhat well. Method 3 shows this same behavior for all the samples.
The same procedure as described above was used for compensated and uncompensated absorption coefficient for "glass wool 100mm". Using uncompensated reflection factors gave, on average, a 0.47% larger absorption coefficient compared to using compensated reflection factors. The word larger rather than different was used in this case as the uncompensated values were always larger. There was not much reason to show an extra figure of the uncompensated absorption coefficients for the glass wool sample as it basically looked identical to 4.16 for Methods 0, 1, and 2.

Figure 4.17 shows the method 0 results from both (a) and (b) in figure 4.15:

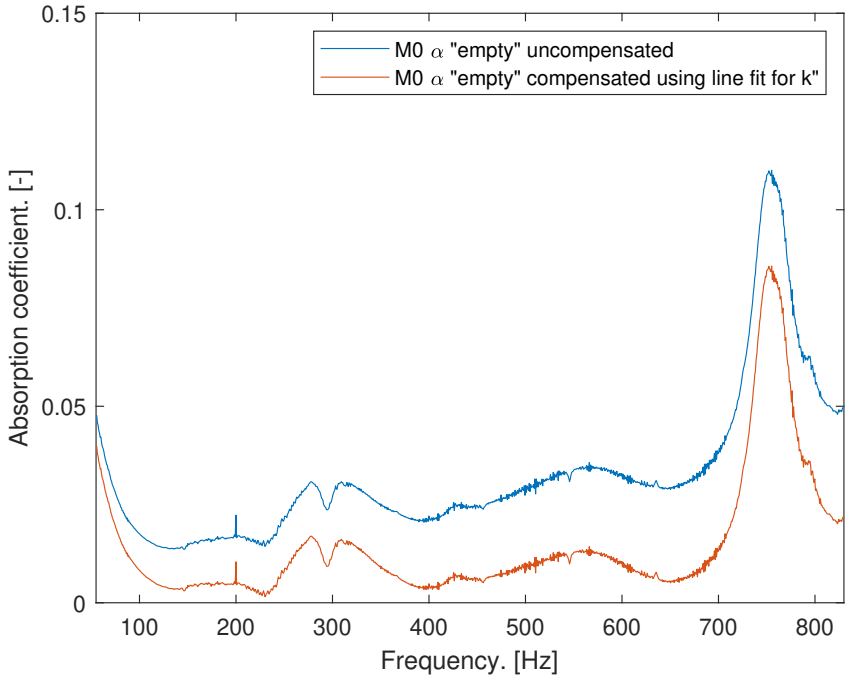

Figure 4.17: Absorption coefficient calculated without compensating for propagation attenuation and calculated using compensated reflection factor for Method 0, sample "empty".

The uncompensated results were calculated to be, on average, 125% larger than the compensated results. This is a substantial error that one can make. It was mentioned earlier that Method 0 uses a microphone 0.64m away from the wall, and were it 0.60m away, it would not require compensation due to propagation attenuation [**3**].
The difference between the most reflective and most absorbing samples used are very large. A potential 0.47% error from the glass wool sample to the incredible 125% potential error for the empty tube when calculating α (nearly at the edge of what is allowed by the ISO to avoid compensation). It is quite straightforward to see that Method 0, described in [**3**] (as well as the Methods based on it, 1 and 2), suffers when calculating absorption factors for highly reflective materials.

To sum up, regarding absorption coefficients:

- On average, there is a 14.9% relative difference between Method 0 and Method 1, for sample "empty".
- On average, there is a 16.3% relative difference between Method 0 and Method 2, for sample "empty".
- On average, there is a 0.13% relative difference between Method 0 and Method 1, for sample "glass wool 100mm".
- On average, there is a 0.18% relative difference between Method 0 and Method 2, for sample "glass wool 100mm".

- On average, Method 0 without propagation attenuation compensation is 125% larger than Method 0 with compensation, for sample "empty".
- On average, Method 0 without propagation attenuation compensation is 0.47% larger than Method 0 with compensation, for sample "glass wool 100mm".

4.6 Influence of Leakage

In figure 3.1, one can see the sample, "smooth rock", in place of where a metal covering would normally be for regular-sized samples that fit in the tube. To have an understanding of what it might look like if the end of the tube was not tightly covered, a simple test was performed. An extra set of 40 measurements, with 5 microphone positions, and 8 sets each for "empty" and "foam 20mm" samples each was performed. In these sets, however, one of the 4 screws used to tighten the metal covering was not screwed in entirely. This resulted in a very small gap, large enough only for a sheet of paper to fit partially through the loose corner. Figure 4.18 shows the comparison of the ISO method with and without leakage:

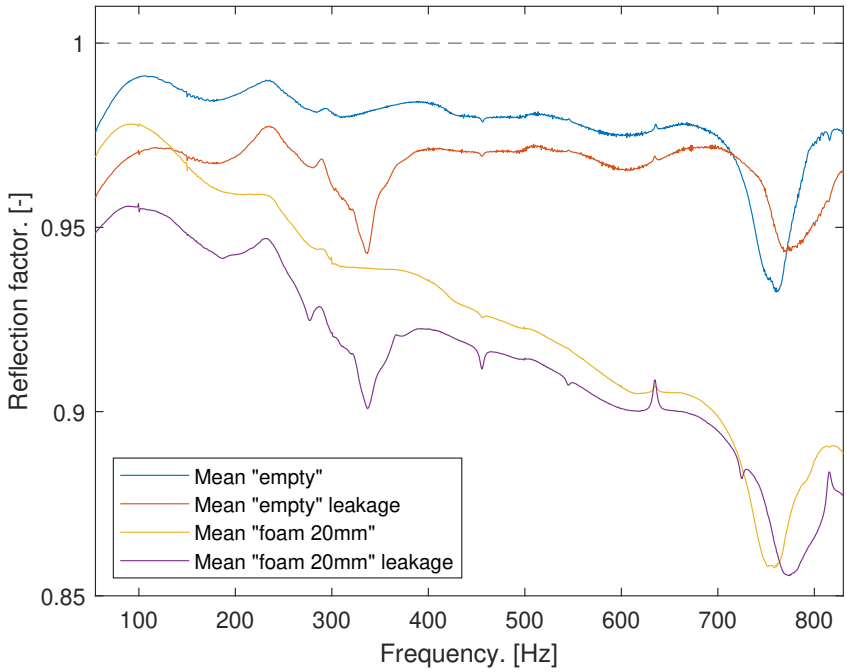

Figure 4.18: Method 0 reflection factors measured properly for "empty" and "foam 20mm", and the same but with a very small gap at the end of the tube.

The y-axis is extended slightly in figure 4.18 to be able to fit sample "foam 20mm". The main reason this was done was due to the suspicious dip in the higher 700-800Hz area. There was a possibility that it could be due to some leakage somewhere along the tube, and this test could provide an insight into what a leak would look like. A somewhat similar dip, in size and shape, to the one in the 700-800Hz area has now been created in the 300-400Hz area. Also of note is that the original dip has been shifted slightly upwards

in frequency as well. One big difference that is not shown in a plot of the mean values of the reflection factor was the much larger variance of results with this introduced leakage. This was especially true in the area around the introduced dip. This can be viewed in appendix A.2. Although one of those measurements had a poor microphone connection, that alone does not seem to be the cause of the increased variance in the difference in results between the leakage and non-leakage reflection factors. This leads one to believe that the original dip in the 700-800Hz frequency range is possibly not due to some unknown leakage. At the same time, however, it is impossible to say this with 100% certainty as there may be certainly still be unknown leaks causing an increased variance in the results along with that dip in the non-leak results. Further work would need to be done to ensure the condition of the tube is without any leaks before drawing that conclusion.

CHAPTER

FIVE

CONCLUSION

Four different Methods were tested in this thesis for calculating reflection factors and absorption coefficients.

- Method 0: ISO 10534-2 (2 mic positions).
- Method 1: Average reflection factor for 5 mic positions using Method 0.
- Method 2: Least mean squares solution for 5 mic positions using Method 0.
- Method 3: Reverberation time in 1 dimension (5 mic positions).

The frequency range considered was 55-830Hz.

Method 3 is the simplest of the Methods in the sense of only actually needing a single microphone position. However, Method 3 is dependent on using Method 0 to calculate the reflection factor for a sample. This is due to the fact that Method 3's calculated reflection factor is the multiplication of the reflection factor for the sample under test and the loudspeaker itself. Being a reverberation time based Method, the results are shown for frequency bands, which makes a comparison to the other Methods not as straightforward. EASERA, the sound analyzing software which gave the reverberation times, only gave reverberation times with two decimals. This may be why frequency bands for lower frequency bands (within the working range) behaved poorly compared to the other Methods. In addition, it was not clear how one would compensate Method 3 for attenuation propagation. Due to these factors and dependency on Method 3 was not considered a strong candidate versus Method 0. Further work in order to consider Method 3 more reliable would be to calculate reverberation times more accurately, find a way to properly compensate for propagation compensation, and look into what causes abnormalities at low-frequency bands.

The influence of propagation attenuation was investigated for Method 0, 1, and 2. Using several microphone positions makes it straightforward to estimate loss due to propagation. When compensating reflection factors using k", non-physical reflection factors for highly

reflective samples were calculated. This was due to k" oscillating in an unexplained manner. In order to avoid non-physical estimates of the reflection factors for highly reflective samples, a line-fit for k" was used instead.

Over the frequency range mentioned, Method 0 had a 70% larger average margin of error than Method 2, which had the lowest error for sample "empty". Method 0 had a 58% larger average margin of error than Method 1, which had the lowest error for sample "glass wool 100mm". Part of this may be due to Method 0 using data from 16 microphone measurements, while Methods 1 and 2 use 40 measurements.

Using reflection factors that were compensated for propagation attenuation using a line-fit for k", the calculated absorption coefficient for the highly reflective empty impedance tube, Methods 1 and 2, had on average (for the 55-830Hz range) a 14.9% and 16.3% relative difference in results, respectively, when compared to Method 0. (The values of each Method's absorption coefficient were not strictly higher or lower, but higher or lower) However, when the same calculation was performed for high absorption sample "glass wool 100mm", the relative difference was reduced to merely 0.13% and 0.18% on average for Method 1 and 2, respectively when compared to Method 0. This highlights that unless one wants to measure highly reflective samples, the potential error being made (assuming Method 1 or 2 is more correct than Method 0) is greatly diminished.
Absorption coefficients using Method 0 were also compared to absorption coefficients using reflection factors from Method 0 that were compensated with a line-fit for k" for propagation attenuation. For the empty tube, uncompensated results were 125% larger than compensated reflection factors. For "glass wool 100mm", the results were only 0.47% larger when using uncompensated reflection factors. To put this into perspective, the maximum distance allowed for a microphone to be away from the wall without needing compensation for propagation attenuation, is three times the maximum lateral dimension, ISO 10534-2 details. This calculates to 0.6m for the impedance tube used. The microphone position used to showcase uncompensated results for Method 0 was positioned at 0.64m. While slightly above the maximum distance, one can say that these results are close to the limit of what would be allowed by ISO 10534-2. This shows a vulnerability of Method 0 when attempting to calculate absorption coefficients for highly reflective materials. Special care should therefore be taken when measuring such materials to be as close to the sample as allowed by the ISO 10534-2 and, in addition, compensate for propagation attenuation to the sample as well. In reality, it may not be possible to measure using the exact microphone positions one would like to due to what the impedance tube one has available is outfitted for. This only strengthens the importance of good compensation for propagation attenuation. On that note, for Methods 0, 1, and 2, finding out more regarding the oscillating effect described in this thesis would allow one to improve upon the method of compensating for propagation attenuation (perhaps not needing to use a line-fit for k". This would aid in calculating reflection factors that are closer to the true value.

BIBLIOGRAPHY

[1] Vorländer, Michael, *Computer Simulations in Room Acoustics: Concepts and Uncertainties*, Acoustical Society of America. 2013.

[2] NS-EN ISO 354, *Acoustics — Measurement of sound absorption in a reverberation room (ISO 354:2003)*. 2003.

[3] NS-EN ISO 10534-2, *Acoustics — Determination of sound absorption coefficient and impedance in impedance tubes Part 2: Transfer-function method (ISO 10534-2:1998)*. 2001.

[4] Hartenstein, Matthieu; Fernandez Grande, Efren; Cutanda Henriquez, Vicente, *An experimental approach for estimating the impedance of elastic non.porous materials.*, Proceedings of EuroNoise. online-pdf 2021.

[5] Blackstock, David T., *Fundamentals of physical acoustics*, John Wiley and Sons. 2000, pp. 298-328.

[6] Penrose, Roger, *A Generalized Inverse for Matrices*, Mathematical Proceedings of the Cambridge Philosophical Society. online-pdf, 1955, pp. 406-413.

[7] Lothar Cremer and Helmut A. Müller, *Principles and Applications of Room Acoustics Volume 1*, Applied Science Publishers. 1984, pp. 229-230.

[8] Heinrich Kuttruff, *Room Acoustics 4th Edition*, Spon Press. 2000, pp. 6.

[9] Vicente Cutanda Henriquez and Peter Juhl, *Matlab code: amb2prop*, 2006 web page (This code references: Rasmussen, K. (1997). *Calculation methods for the physical properties of air used in the calibration of microphones. online-pdf*, where the formulas used in the code are from)

[10] Harris, Cyril M., *Absorption of Sound in Air versus Humidity and Temperature*, The Journal of the Acoustical Society of America. 1966, pp. 148-157.

APPENDIX

A

APPENDIX

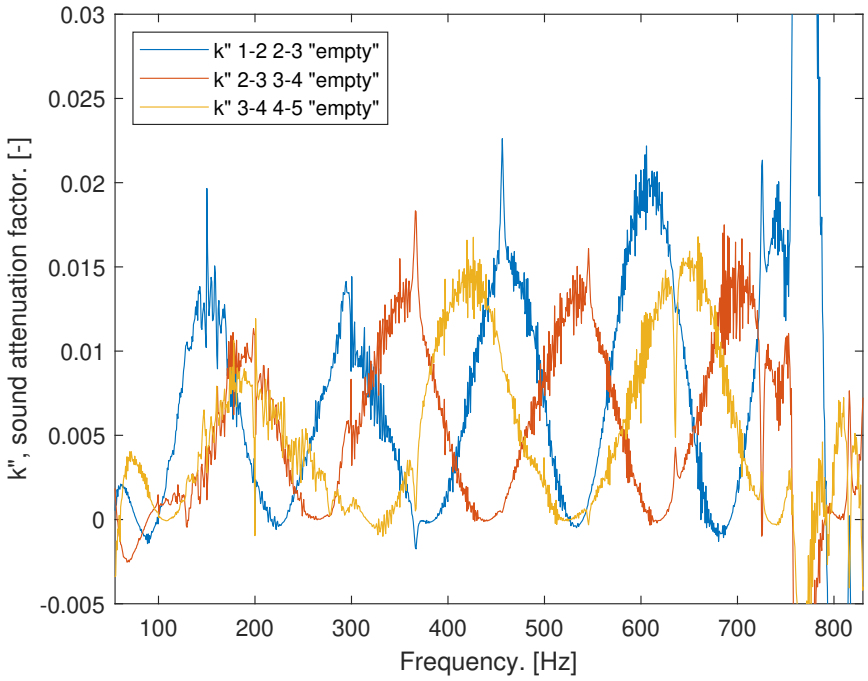

Figure A.1: Sound attenuation factor from all microphone pairs that share a common microphone, sample "empty" Method 0.

In figure A.1, it is possible to see some sort of relationship between the distance the microphone pairs being used are placed away from the wall and the frequency of oscillation.

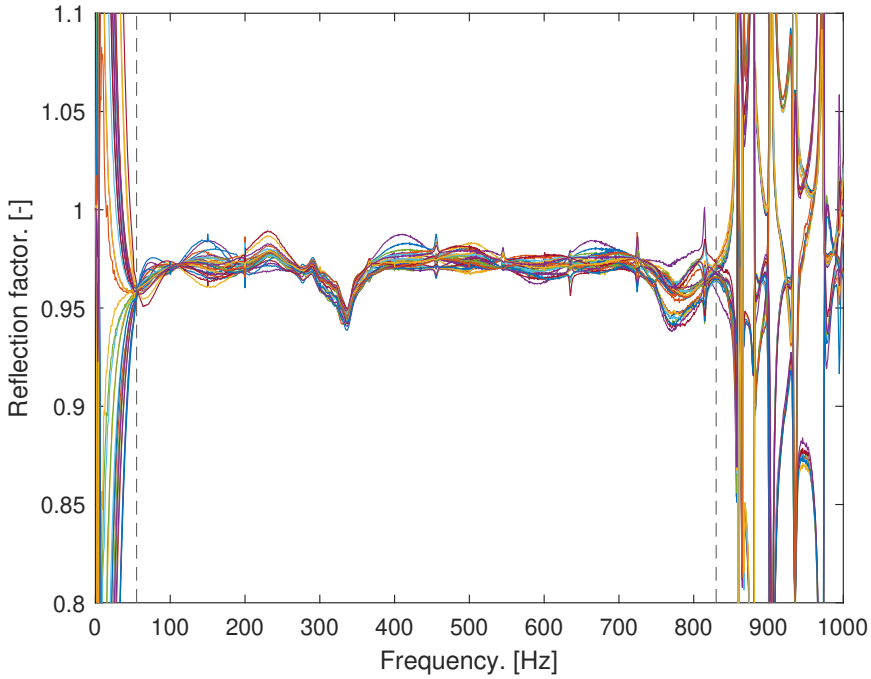

Figure A.2: Reflection factor measurements for sample "empty" similar to 4.1 but with leakage introduced.

One measurement used for calculating the reflection factor in appendix A.2 had a poor connection. This can be easily identified as the top reflection factor at 770Hz, as this faulty measurement has caused a very out of place reflection factor. The introduced dip is noticeably located around 330Hz, and the results in general seem quite a bit more noise than in figure 4.1.

The equipment used in the experiments are listed in the following table A.1:

Table A.1: List of equipment used

Equipment	**Manufacturer**	**Type number**
Microphone	Bruel & kjaer	4190
Microphone pre-amp	Norsonic	NOR 1201
Microphone amplifier	Bruel & kjaer	1708
Sound card	Roland	Studio-capture UA-1610
Loudspeakers	NTNU	unknown
Loudspeaker amplifier	NAD	312
Sound analyzing software	EASERA	v1.2.13

NTNU

Norwegian University of
Science and Technology